

AD-A233 013

REPORT DOCUMENTATION PAGE

Form Approved
OMB No. 0704-0188

Public reporting burden for this collection of information is estimated to average 1 hour per response, including the time for reviewing instructions, searching existing data sources, gathering and maintaining the data needed, and completing and reviewing the collection of information. Send comments regarding this burden estimate or any other aspect of this collection of information, including suggestions for reducing this burden, to Washington Headquarters Services, Directorate for Information Operations and Reports, 1215 Jefferson Davis Highway, Suite 1204, Arlington, VA 22202-4302, and to the Office of Management and Budget, Paperwork Reduction Project (0704-0188), Washington, DC 20503.

| | | | |
|--|---|--|------------------------------------|
| 1. Agency Use Only (Leave blank). | 2. Report Date. 1990 | 3. Report Type and Dates Covered. Contract | |
| 4. Title and Subtitle. Prototype development of an Expendable Light Scattering Sensor | | 5. Funding Numbers. Program Element No. 63704N Project No. R01180S Task No. 300 Accession No. DN250053 | |
| 6. Author(s). J. Ronald V. Zaneveld and Robert Bartz | | 8. Performing Organization Report Number. DTIC FILE COPY | |
| 7. Performing Organization Name(s) and Address(es). Sea-Tech, Inc. P. O. Box 779 Corvallis, OR 97339 | | 10. Sponsoring/Monitoring Agency Report Number. CR 018:91 | |
| 9. Sponsoring/Monitoring Agency Name(s) and Address(es). Naval Oceanographic and Atmospheric Research Laboratory* Ocean Science Directorate Stennis Space Center, MS 39529-5004 | | 11. Supplementary Notes. Contract N00014-90-C-6012 | |
| 12a. Distribution/Availability Statement. Approved for public release; distribution is unlimited. *Formerly Naval Oceanographic and Atmospheric Research Laboratory | | 12b. Distribution Code. S D | |
| 13. Abstract (Maximum 200 words). The technical objective of the proposal was to evaluate a device that could eventually be used for the in situ measurement of particle concentration in an aircraft-launched expendable mode. The following criteria had to be met: 1) Scientifically justifiable measurement, 2) Sufficient accuracy for oligotrophic regions (i.e. 1 μ g/l particle resolution), 3) Deployment from existing shipboard delivery systems, 4) low cost. We constructed and tested a light scattering device that met all criteria. Based on first principles we derived a transfer function for the device that compared well with observation. The device was tested in the laboratory and was shown to have a resolution in excess of 1 μ g/l and a full scale range of 5 mg/l. Complete electronics of the device and the deployment system were constructed and tested in the laboratory. Sea tests of the sensor were carried out in both turbid coastal water and clear oceanic waters, showing that the scattering sensor has approximately the same sensitivity and range as the standard Sea Tech 25 cm pathlength transmissometer. The output of the scattering sensor cannot be given in absolute terms, however. The research thus showed that the construction of aircraft-launched expendable scattering sensors is feasible. | | | |
| 14. Subject Terms. (U) Oceanography; (U) Optical Instruments; (U) Engineers | | 15. Number of Pages. 37 | 16. Price Code. |
| 17. Security Classification of Report. Unclassified | 18. Security Classification of This Page. Unclassified | 19. Security Classification of Abstract. Unclassified | 20. Limitation of Abstract. SAR |



EA TECH INC. FAX 503-757-7027 TELEX 258519 CTEK
P.O. Box 779 • Corvallis, Oregon 97339 • 503-757-9716

FINAL REPORT
TO
NOARL

Contract No: N00014-90-C-6012

TITLE:

Prototype Development of an Expendable
Light Scattering Sensor

DATE:

12 DECEMBER 1990

J. Ronald V. Zaneveld
J. Ronald V. Zaneveld
Principal Investigator

Robert Bartz
Robert Bartz
President

| | |
|--------------------|--------------------------|
| Accesion For | |
| NTIS | CRA&I |
| DTIC | TAB |
| Unannounced | <input type="checkbox"/> |
| Justification | |
| By | |
| Distribution / | |
| Availability Codes | |
| Dist | Avail and/or Special |
| A-1 | |



91 3 20 093

FINAL REPORT TO NOARL
EXPENDABLE PARTICLE SENSOR

TECHNICAL ABSTRACT

micro *micro*

The technical objective of the proposal was to evaluate a device that could eventually be used for the *in situ* measurement of particle concentration in an aircraft-launched expendable mode. The following criteria had to be met: 1) Scientifically justifiable measurement, 2) Sufficient accuracy for oligotrophic regions (i.e. 1 $\mu\text{g/l}$ particle resolution), 3) Deployment from existing shipboard delivery systems, 4) low cost. We constructed and tested a light scattering device that met all criteria. Based on first principles we derived a transfer function for the device that compared well with observation. The device was tested in the laboratory and was shown to have a resolution in excess of 1 $\mu\text{g/l}$ and a full scale range of 5 mg/l. Complete electronics of the device and the deployment system were constructed and tested in the laboratory. Sea tests of the sensor were carried out in both turbid coastal water and clear oceanic waters, showing that the scattering sensor has approximately the same sensitivity and range as the standard Sea Tech 25 cm pathlength transmissometer. The output of the scattering sensor cannot be given in absolute terms, however. The research thus showed that the construction of aircraft-launched expendable scattering sensors is feasible.

47

INTRODUCTION

Presently, a low cost expendable sensor for the measurement of suspended particle concentration in water does not exist. Such a sensor is desirable to provide a low-cost means of acquiring near-synoptic data for suspended particle concentrations in the sea. The particle sensor must operate in daylight or dark. The sensor must have adequate sensitivity to measure particle concentrations as low as 5 $\mu\text{g/l}$, this requires a resolution of at least 1 $\mu\text{g/l}$ in order to delineate vertical structure in oligotrophic regions. Ideally, the sensor would be compatible with existing airborne and shipboard hardware used to deploy other expendable devices. In this document we will report the research that was carried out during this contract to demonstrate the feasibility of such a sensor.

The measurement of suspended particulate matter in water has far-reaching applications. The suspended particulates are comprised of both organic and inorganic material, and these particles are indicators of biological, chemical and geological processes in the ocean. Suspended particle concentration varies from approximately 5 $\mu\text{g/l}$ in the cleanest ocean water to several hundred mg/l in very turbid water.

In the past several years, optical and acoustic schemes have been used to measure suspended particulate matter in water. Because of the high correlation between the light transmission and total suspended mass, the transmissometer has emerged as the best instrument to measure suspended particle concentrations in the ocean. A modern light emitting diode (LED) transmissometer developed by Bartz *et al.* (1978) more than a decade ago, has, over years of use, proven to be a very sensitive and stable tool for the determination of suspended particle concentrations in water. Transmissometers today are used world wide in profiling, moored, and towed modes to assess the concentration of particulate matter in water. While providing high accuracy for profiling, they do require use of an oceanographic winch and a CTD or other instrument platform. Profiling is expensive in terms of ship time and this limits the number of profiles that can be obtained on any given cruise, reducing the synopticity of data sets.

As a result of recent oceanographic work such as in ODEX, BIOWATT, Warm Core Rings, ML-ML, the need for a rapid, nearly-synoptic assessment of the particle field has become clear. As more research effort is expended on the linkage between physical and biogeochemical features of the world ocean, a means for the simultaneous rapid measurement of physical and biogeochemical parameters must be developed. An obvious example of such a physical sensor is the airborne expendable bathythermograph or AXBT. It is our goal to develop a similar optical sensor that will measure particulate matter concentration in water with a sensitivity of 1 $\mu\text{g/l}$.

The technical objectives of the proposal were to evaluate a low cost, expendable device for the *in situ* measurement of particle concentration. The following criteria had to be met.

- 1) Scientifically justifiable measurement
- 2) Sufficient accuracy for oligotrophic regions (i.e. 1 $\mu\text{g/l}$ particle resolution)
- 3) Deployment from existing shipboard delivery systems

Development, laboratory and sea tests of the 650 nm forward scattering sensor were funded by NOARL with the ultimate aim of developing an air-launched expendable sensor that could be used to obtain the diffuse attenuation coefficient from inherent properties. Sea Tech, Inc. was also funded by the Office of Naval Research to do research and develop an expendable sensor that could be used to determine suspended particle profiles in the ocean. Significant improvements in the design of the forward light scattering sensor were made based on experience gained from the NOARL scattering sensor development. Results are presented in a final report to ONR. The ONR program has the ultimate aim of developing a ship-launched device. Sea Tech Inc together with Sparton of Canada have submitted a Phase II proposal to ONR for the development of a ship-launched expendable particle sensor. Additional funding will be required to develop an air-launched expendable particle

sensor. This will involve modification of the ONR ship-board probe such that data transmission is accomplished via a sea surface VHF transmitter and a airborne receiver. Sea Tech Inc. and Sparton of Canada will also submit a proposal to NOARL for the development of an air-launched optics sensor.

Concentration of suspended matter is a major parameter in the determination of optical properties, so there will be considerable technology and research transfer from the ONR Phase II program to the NOARL program. Since the requirements for the air-launched and ship-launched devices are different we will need additional funding to develop the air-launched device. We also need to point out that the development of the air-launched device funded by NOARL is dependent upon funding of the Phase II proposal by ONR. Finally, the additional funds requested from NOARL to develop the air-launched capability will be \$200,000 over a two year period.

SCIENTIFIC ANALYSIS OF THE SENSOR DESIGN

Numerical analysis of the sensor was carried out to evaluate the response to various types of particles and to determine the potential response to particulate concentration changes.

It is clear that if the nature (size, shape and index of refraction distributions) of the particulates do not change, the particulate optical properties will scale linearly with the total particle concentration (Zaneveld, 1973). Any scattering measurement will thus be proportional to total suspended mass provided the particulate nature does not change. If the particulate nature changes with depth, it has been shown (Morel, 1973; Bricaud et al., 1983) that backscattering is more dependent on particulate properties (especially shape) than total or forward scattering.

Numerical evaluation of the sensitivity of a forward scattering sensor was carried out. The design of the forward scattering sensor consists of a light emitting diode (LED) light source in the red part of the spectrum. Coaxially aligned with the light source is a silicon detector and filter, optically separated from the light source by a light stop. Figure 1 shows a drawing of the forward scattering sensor as well as the sample volume. Direct light cannot reach the detector. The filter in front of the detector reduces the influence of ambient light.

Figure 1 shows a diagram of the expandable scattering sensor. Each element of the sample volume scatters light from the light source to the detector at an angle determined by its location. The elementary volume dV is located a distance y from the detector and a distance h from the line connecting the centers of the light source and detector. This centerline has a length of R . x forms an angle θ with the centerline and y forms an angle ϵ . dV is rotated an angle ϕ relative to the vertical. A is the area of the detector and c is the beam attenuation coefficient. Referring to Figure 1, it can then be seen that the power received at the detector, P_{out} , from the volume element, dV , is given by

$$P_{out} = \int_{\phi_{mn}}^{\phi_{mx}} \int_{\theta_{mn}}^{\theta_{mx}} \int_{\epsilon_{mn}}^{\epsilon_{mx}} \beta(\theta + \epsilon) L(\theta) \frac{e^{-cx(\theta)}}{x^2(\theta)} \frac{A e^{-cy(\epsilon, \theta)}}{y^2(\epsilon, \theta)} dV(\epsilon, \theta, \phi) \quad (1)$$

where β is the volume scattering function, L is the radiance distribution of the light source, and the subscripts mx and mn refer to the maximum and minimum values of the angles, which are determined by the geometry. The volume element is given by

$$dV(\epsilon, \theta, \phi) = \frac{x(\theta, \epsilon) y(\theta, \epsilon)}{\sin(\theta + \epsilon)} d\theta d\epsilon h d\phi. \quad (2)$$

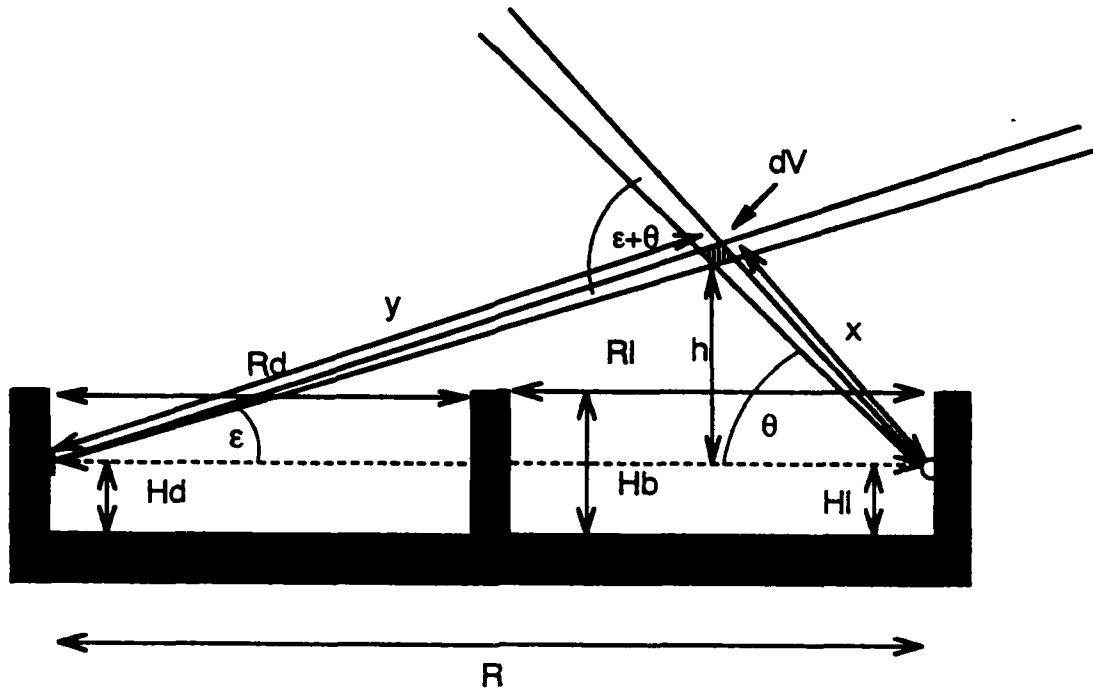


Figure 1. Diagram of Expendable Scattering Meter

Substituting for h and rewriting the equation in terms of ϵ , θ , and ϕ gives:

$$dV(\epsilon, \theta, \phi) = \frac{x(\theta, \epsilon) y(\theta, \epsilon) R \tan \theta \tan \epsilon}{\sin(\theta + \epsilon) \tan \theta + \tan \epsilon} d\theta d\epsilon d\phi. \quad (3)$$

Insertion into equation 1 produces:

$$P_{out} = \int_{\phi_{mn}}^{\phi_{mx}} \int_{\theta_{mn}}^{\theta_{mx}} \int_{\epsilon_{mn}}^{\epsilon_{mx}} \beta(\theta + \epsilon) L(\theta) \frac{e^{-\alpha(\theta)} A e^{-cy(\epsilon, \theta)}}{x(\theta) y(\epsilon, \theta)} \frac{R \tan \theta \tan \epsilon}{\tan \theta + \tan \epsilon} \frac{d\theta d\epsilon d\phi}{\sin(\theta + \epsilon)} \quad (4)$$

where x and y are given by

$$x(\theta, \epsilon) = \frac{R \tan \epsilon}{\cos \theta (\tan \theta + \tan \epsilon)} \\ y(\theta, \epsilon) = \frac{R \tan \theta}{\cos \epsilon (\tan \theta + \tan \epsilon)}. \quad (5)$$

For light passing over the round top of the block, which is equivalent to the condition

$$\phi \leq \frac{\pi}{2}, \quad (6)$$

the lower limit of integration for theta is determined from a numerical solution to the following set of equations using the Mathematica application. This accounts for the refraction by the lens of the LED resulting in an offset from the axis of the starting point of the light ray.

$$\begin{aligned}
x &= 31 \\
y &= 3 \\
y_1 &= \text{Sqrt}[0.0001 - x^2] \\
a &= \text{ArcTan}[x/ \text{Sqrt}[0.0001 - x^2]] \\
b &= \text{ArcTan}[y_1/(x + 0.009146)] \\
c &= \text{Pi}/2 - a - b \\
q_{mn} &= \text{ArcTan}[(y - y_1)/(x - x_1)] \\
d &= \text{Pi}/2 - a - q_{mn}
\end{aligned}$$

$$\text{FindRoot}[\text{Sin}[d] == 1.1278 * \text{Sin}[c], \{x_1, 0.001\}] \quad (7)$$

For light passing to the side of the block, the lower limit of integration for theta is

$$\theta_{mn} = \tan^{-1} \left[\frac{0.0025}{R \cos \left(\frac{\pi}{2} - \phi \right)} \right]. \quad (8)$$

In a similar way we determined the lower limit of integration for ϵ . Upper limits are defined by the radiance distribution of the light source and the detector characteristics.

In order to predict the sensitivity of the scattering sensor, we have applied the mathematical analysis of the sensor to the clearest ocean water. We used the shape of the scattering function obtained by Petzold (1972) in the Tongue of the Ocean in the Bahamas (Station AUTEC 9). The other parameters are obtained from the characteristics of the sensor as given in the following table.

| | |
|----------------------------------|--|
| Total Length | 6.0 cm |
| Light to Block | 2.5 cm |
| Detector to Block | 3.1 cm |
| Axis Height | 4.5 mm |
| Block Height | 7.5 mm |
| Block Width | 6.0 mm |
| Radiance Range | 2 to 5 mW/ster. |
| Half Power Angle of Light Source | 12 degrees in air, 23 degrees in water |

In general the relationship between the particulate beam attenuation coefficient ($c - c_{\text{water}}$), c_p , and suspended mass depends on the particle size distribution and index of refraction. Spinrad (1986) has derived a calibration diagram of c_p per unit volume of suspended matter as a function of size distribution slope and index of refraction. For many naturally occurring particles we find that we can use the relationship that $c_p = 1 \text{ m}^{-1}$ corresponds to approximately $1000 \mu\text{g/l}$ (for example Spinrad et al., 1983). In the following discussions we have thus assumed that when $c_p = 0.001 \text{ m}^{-1}$, this corresponds to approximately $1 \mu\text{g/l}$. This allows us to use the beam attenuation meter to calibrate the scattering sensor in terms of suspended mass. It also allows us to select a beam attenuation coefficient for clear natural water. This was obtained by adding $10 \mu\text{g/l}$ of suspended mass to pure water. Since pure water has a c of 0.364 m^{-1} , and the suspended mass has a c_p of approximately 0.010 m^{-1} (see above discussion), we set the beam attenuation for clean natural water at $c = 0.374 \text{ m}^{-1}$.

Using the equations and parameters described in this section, the calculated power received for the clean water is between 2.1×10^{-11} and $5.2 \times 10^{-11} \text{ W}$ which is at least one order of magnitude above the noise level of the detector. The range in output power values is generated by the range in radiance specified by the manufacturer of the LED. Referring to the scattering sensor electronic schematic, figure 7, the silicon detector has a sensitivity of 0.4 amps/watt at 650 nm, and the current to voltage converter, U5 uses a $2 \text{ M}\Omega$ resistor, R8. The electronics, U5 and U6 then amplifies the output of the current to voltage converter with a voltage gain of 625.

The scattering sensor voltage output, E_{out} can now be determined for the clean water since,

$$E_{out} = [(\text{Power Received, watts}) \times (\text{Detector Sensitivity, 0.4 amps/watt})] \times [(\text{current to voltage conversion, } 2 \times 10^6 \text{ volts/amp}) \times (\text{voltage gain, 625})]$$

Substitution of the calculated power out into the above equation shows that the sensor output, E_{out} for the clean water is 10-26 mV. The sensor electronic noise with a 1 second time constant is approximately 1 mV, so that in the clearest ocean water, (10 $\mu\text{g/l}$) we have a signal to noise ratio in the range of 10 to 26.

If we use the minimum specified LED output we see that 10 $\mu\text{g/l}$ of suspended material gives a scattering signal of approximately 10 mV. We can conclude that the worst case sensor sensitivity for the measurement of suspended mass will be approximately 1 $\mu\text{g/l}$. For the entire LED output range we get from 1.0 to 2.6 mV/ $\mu\text{g/l}$. Experimental results are given in the section on laboratory and field tests (figure 24), and show that the range of sensitivity for two types of particulate matter (organic and inorganic) is 0.91 to 1.68 mV/ $\mu\text{g/l}$. This confirms that the previous calculations are reasonably accurate. The analysis thus demonstrates that we have sufficient signal even in the clearest ocean waters. The analysis furthermore shows that an adequate transfer function for the device has been derived from first principles, as the theoretical and experimental results correlate well.

The analysis also enabled us to measure the relative sensitivity of the device as a function of scattering angle (Figure 2.). A typical volume scattering function was used to derive the signal received due to scattering at each angle. The maximum sensitivity is at 17° scattering angle. While smaller angles would have a higher volume scattering function, little sample volume is exposed from which light scattered at those angles could reach the receiver. The half power range is from 12.5° to 26°. About 14% of the total scattering coefficient for a typical ocean volume scattering function falls in that range.

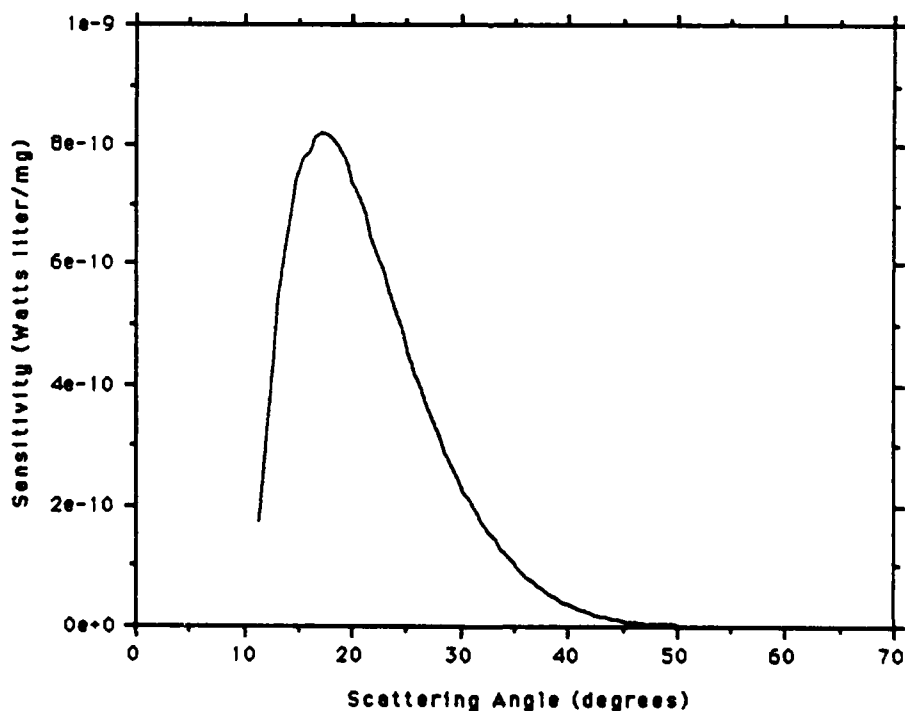


Figure 2. Sensitivity of the 650 nm sensor as a function of scattering angle.

OPTICAL, MECHANICAL AND ELECTRONIC DESIGN

During the design phase of this expendable forward light scattering sensor project, Sea Tech has focused mainly on the scattering sensor design, development and test.

Sea Tech has also considered the design of a deployment system that will be required to field test this sensor. First, a low cost expendable data transmission system is necessary to acquire the data and transmit it over a sea link to a data receiver. A data receiver, data decoder, and computer are then needed to process, display and archive the data. The measurement of temperature and depth is also highly desirable and will require multiplexing sensor outputs.

In the following text we will first describe the scattering sensor development and test. Then a depth sensor design is presented. Finally, the deployment system design and prototype testing is described.

The long range goal of this initial work, is to eventually develop an airborne system that will obtain a suspended particle profile in the sea. We also intend to measure temperature and depth with the same probe. For this reason the forward light scattering sensor system will be referred to in the following text as an airborne expendable optical, temperature and depth sensor system, (AXOTD). The primary goal of this development was to design a viable scattering sensor and test the device in a ship-board environment. No work has been done or is reported that addresses the airborne VHF transmitter or receiver.

Forward Scattering Suspended Particle Sensor

The mechanical design of the NOARL scattering sensor is shown in figure 3 and the optical design is shown in figure 4.

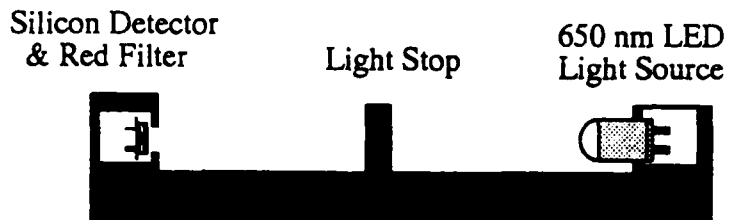


Figure 3, Side view of the NOARL forward light scattering sensor, actual size.

The mechanical design of the forward light scattering sensor is very simple, a light emitting diode, (LED) and silicon detector face each other on a black plastic rail with a light stop half way between. The optical design of the forward scattering sensor is shown in figure 4. The LED projects light around the light stop in the direction of the silicon detector. The detector is placed behind a red filter to prevent saturation in ambient light. The light stop prevents any direct light from entering the detector, thus only light scattered in the direction of the detector is measured. The scattered light measured is proportional to the suspended particle concentration in water.

The half power beam width of the LED is approximately 23° in water. The ray traces demonstrate that the sensitive volume includes scattered light from the near forward to over 90 degrees. This diagram is a bit misleading because the volume scattering function is strongly peaked in the forward direction. This means that most of the light measured will be scattered close to the light stop. The calculated sensitivity as a function of angle for the sensor is shown in figure 2. The angle of maximum sensitivity was shown to be 17 degrees.

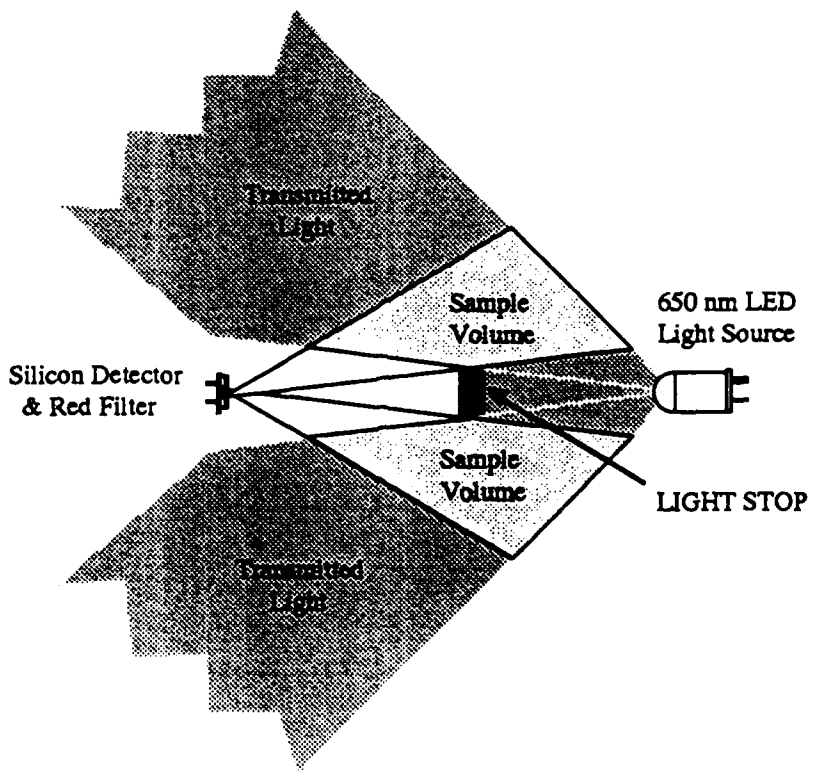


Figure 4, Scattering sensor optical diagram, top view

A non-expendable prototype instrument was constructed that could be tested in both the laboratory and the field. This instrument is shown in figure 5. The electronics for the light scattering sensor were installed in the pressure case and the scattering sensor attached to the end cap as shown.

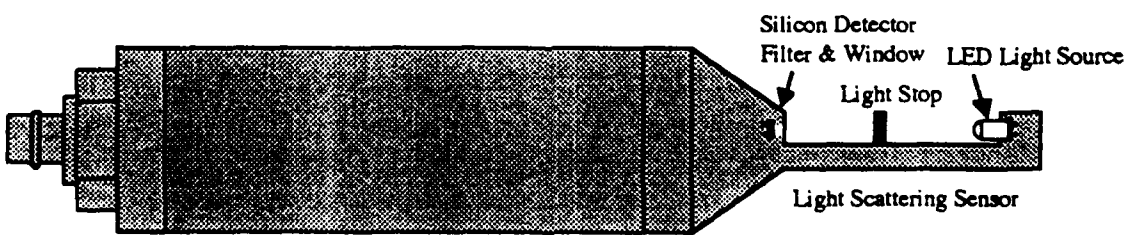


Figure 5, Packaged Sensor Design

A printed circuit board was laid out and fabricated to test the scattering meter. The layout of the printed circuit board is shown in figure 6.

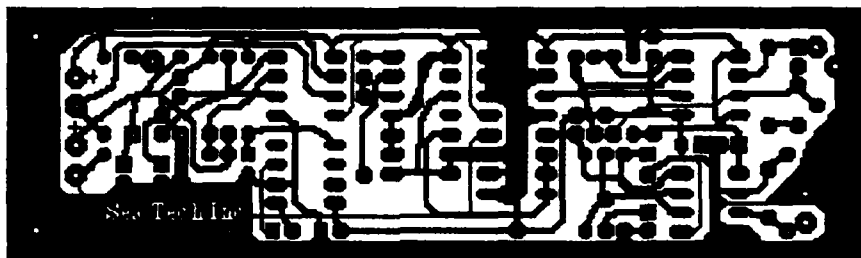


Figure 6, Scattering sensor printed circuit board layout.

A schematic diagram of the forward scattering sensor electronics is shown in Figure 7. The operation of the light scattering sensor is as follows: The LED is modulated at 500 Hz and driven with 30 millamps of current, resulting in a power output of approximately 2 to 5 milliwatts / steradian. The light receiver is a 1.23 mm² silicon detector equipped with a daylight filter to prevent detector saturation in ambient light. The sensitivity of the light detector is approximately 0.4 amps / watt at 650 nm wavelength.

The modulated light scattered from the sample volume is measured by the signal detector, converted to a voltage, amplified and then synchronously detected. The synchronous detector is followed by an adjustable gain, adjustable offset, low pass filter. The low pass filter time constant is 1 second. The output of the low pass filter ranges from 0 to 5 VDC. The system gain was set so that full scale, 5 VDC, would correspond to 5 mg/l.

Deployment System Design

The deployment system will contain three major components.

- (1) Expendable Probe Launcher
- (2) Expendable Probe, AXOTD
- (3) Computer Interface Card & Software

The deployment system design focused on the low cost expendable multichannel data acquisition system that will transmit data to a computer over a two wire sea link. Sea Tech has designed and tested the critical elements of this system to define overall system specifications.

Specifications of major interest are: A scattering sensor resolution of 1 $\mu\text{g/l}$ and full scale range of 5 mg/l. Temperature sensor resolution should be approximately 0.01 $^{\circ}\text{C}$ with a range -5 $^{\circ}\text{C}$ to 35 $^{\circ}\text{C}$. Depth accuracy using drop rate should be 2% and needs to be validated by using a pressure transducer.

The system performance will be constrained by the limited bandwidth of the two-wire transmission line used for the sea link. In this design we evaluated a 500 meter transmission line giving a maximum probe depth of 500 meters. Due to the limited bandwidth, a sample rate of two samples / second was chosen providing one meter depth resolution using a probe drop rate of 2 m/sec.

In the following text we will describe the system that was designed and tested to process the data from AXOTD in a ship-board environment.

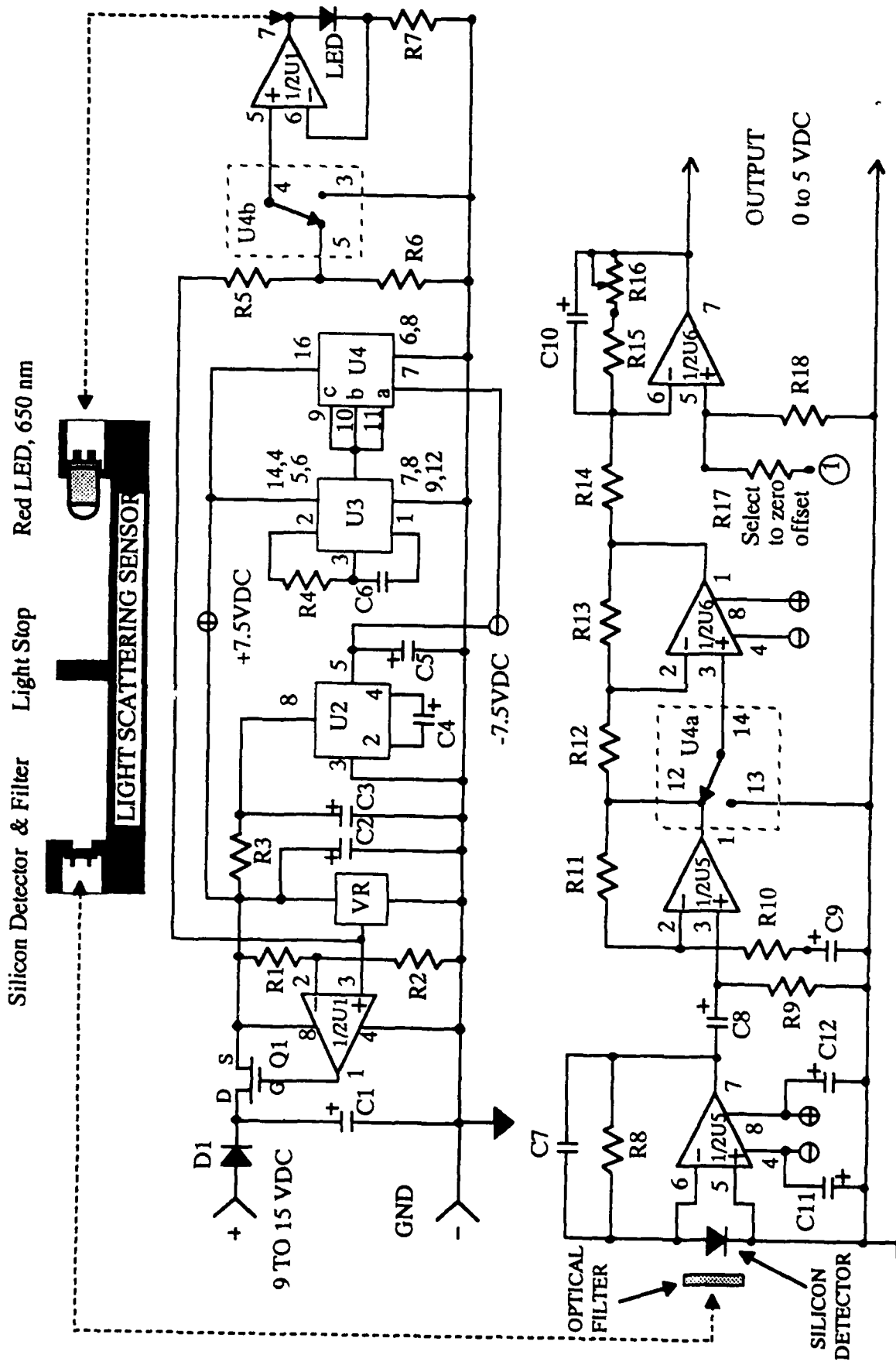


Figure 7, Light Scattering Sensor Schematic

1) Probe Launcher

In order to minimize costs and maximize eventual use, the Sparton of Canada, (S.O.C.) or Sippican deployment system will be used to launch the AXOTD into the sea. The Launcher is designed to launch an expendable probe that uses a two wire sea link and is approximately 2 inches in diameter and 15 inches long.

2) Expendable Probe, AXOTD

The expendable probe consists of the following components:

- (2a) Transmission Line
- (2b) Suspended particle sensor
- (2c) Optional depth sensor
- (2d) Temperature sensor
- (2e) Telemetry system
- (2f) Seawater switch
- (2g) Battery power source
- (2h) Sensor Housing & Weight
- (2i) Tail fin & wire spool

A conceptual mechanical design of the AXOTD probe without the tail fin and wire spool is shown in Figure 8. It is 2 inches in diameter and 5.5 inches long. These dimensions are compatible with the existing S.O.C. / Sippican launcher.

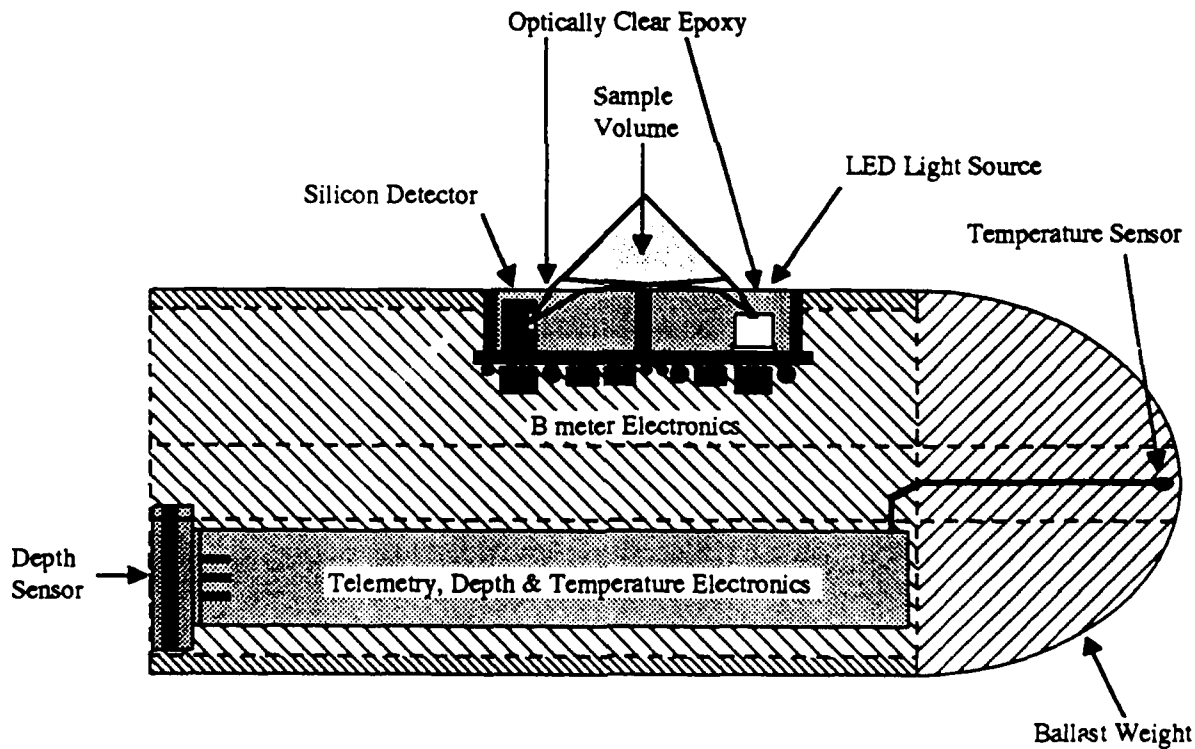


Figure 8, AXOTD Sensor Mechanical Design

A block diagram of the AXOTD electronics is shown in Figure 9. Each component of this block diagram is described in the following text.

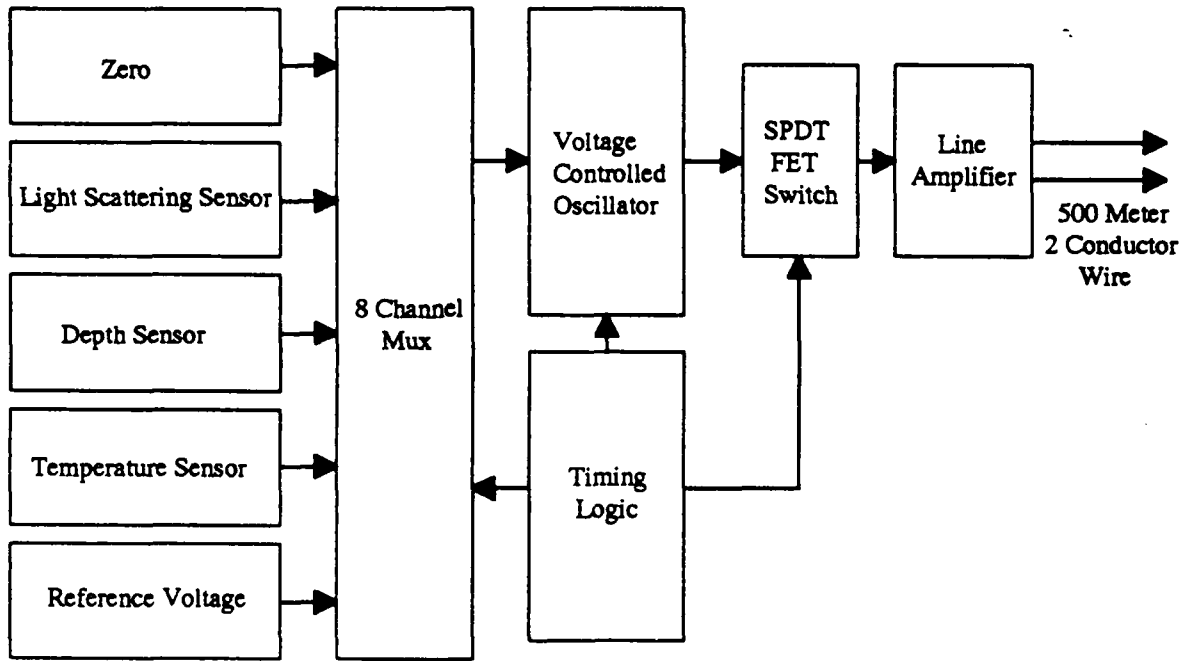


Figure 9, AXOTD Sensor block Diagram

2a) Transmission line

System performance is constrained by the length of the two wire transmission line. The signal loss due to limited bandwidth of the two wire transmission line is shown in Figure 10 and imposes severe constraints on the signals which are transmitted from the AXOTD to the receiver in the computer interface card. The data shows that at 500 meters reasonable bandwidth can be expected and at 3000 meters bandwidth is severely restricted. The high DC resistance of the wire ($2.625\Omega/\text{meter}$) makes it impractical to transmit analog voltages to the receiver. The high electrical capacitance, (0.65 nF/meter) of the wire pair causes severe attenuation of signals as a function of frequency. In addition the wire will act as an antenna to pick up electrical noise at all frequencies, causing interference and increased noise levels at the receiver.

Considering all the above, the 500 meter two wire transmission cable was modeled as shown in figures 10, and 11 and transmission frequency and bandwidth were chosen to optimize resolution, sample rate, and surface signal recovery. Considering 7 dB loss to be the maximum attenuation desired, the data in figure 10 shows that the bandwidth can be 1 KHz centered at 1 KHz. This results in a lower frequency of 500 Hz and an upper frequency of 1500 Hz.

Based on previous experience and extensive computer modeling and transient analysis, we chose to transmit data over the sea cable using a triangle waveform. The triangle waveform is generated by the VCO and buffered by a line amplifier to differentially drive the 500 meter sea cable. The triangle waveform has several advantages over square waves in this environment. Since this waveform has a much lower percentage of high-order harmonics, less power is lost to capacitive loading by the wire. In addition, the triangle wave will suffer less distortion, allowing more precise frequency determination by the receiver. The ideal waveform would be a sine wave; however the circuitry to generate sine waves is more expensive and requires substantially more power.

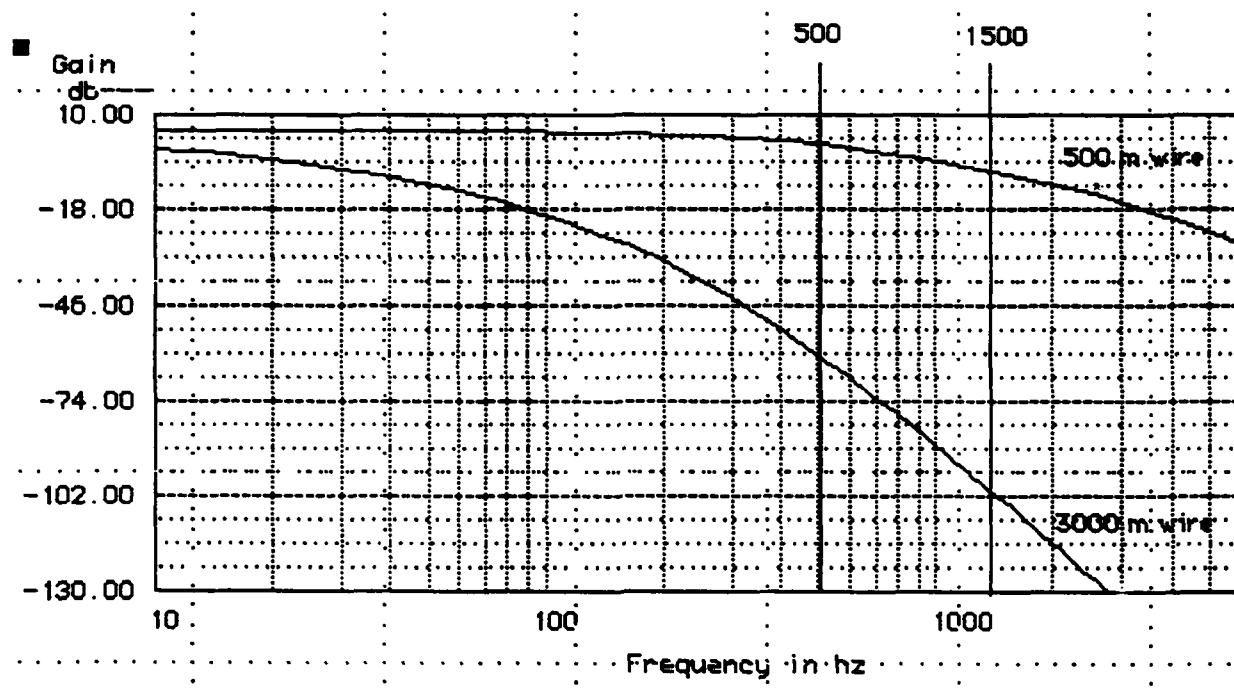


Figure 10, Comparative Line Gains for 500m wire and 3000m wire. Over the range from 500 to 1500Hz, the gain for the 500m wire changes by 7dB while the gain for the 3000 meter wire changes by more than 38dB. At 1500Hz, the signal levels differ by more than 100dB.

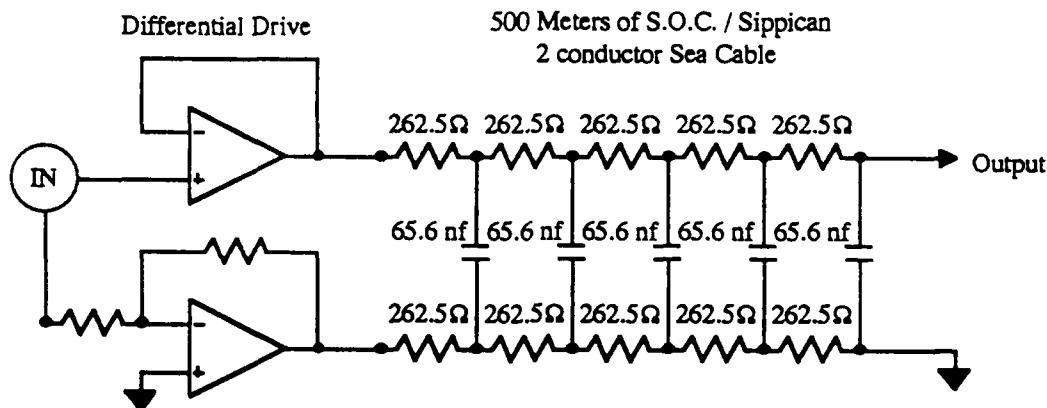


Figure 11, Line driver and 500 meter transmission line

2b) Suspended Particle Sensor

A conceptual mechanical design of the AXOTD probe that could be implemented in an airborne application is shown in figure 8. The design of the forward scattering suspended particle sensor was described in a previous section. The design shown in figure 3 could be easily modified to implement the conceptual design shown in figure 8.

2c) Depth sensor

A 100 meter full scale depth sensor will be included in prototype units to verify sensor drop-rate. At present the depth is determined by the rate at which the sensor falls through the water column. This scheme limits accuracy to about 2% at best and is difficult to verify. We have evaluated a low cost depth sensor that can be included in a prototype design to determine sensor drop rate. An outline drawing of the prototype depth sensor developed is shown in figure 12. The depth sensor schematic diagram is shown in figure 13

At this time we do not plan to include a depth sensor in the final design. Depth sensors are still quite expensive and require calibration to obtain the required depth accuracy. Incorporating a depth sensor in the final design would also significantly increase the cost of an airborne probe.

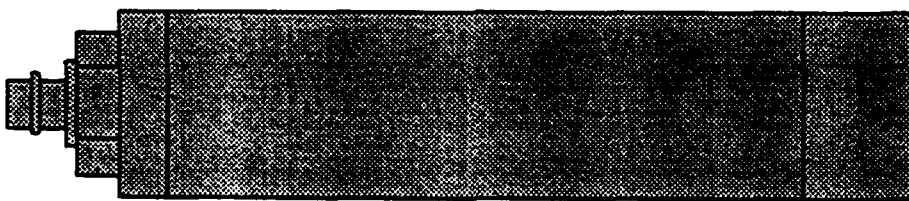


Figure 12, Depth sensor outline drawing

2d) Temperature sensor

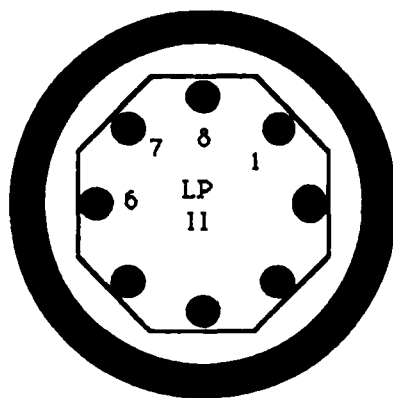
A temperature sensor will be included in the AXOTD since the relationship between particle profiles and temperature profiles will be very important. Temperature is a major mechanism in the generation of density gradients and therefore stratification of particulate matter. With follow-on funding we plan to develop electronics that uses the low cost S.O.C. temperature sensor in this expendable probe.

2e) Telemetry system

The telemetry system design is shown in figure 14. The telemetry system is used to measure the multiplexed signals from the three sensors and transmit serial data over the 500 meter wire. In this design we use time-division multiplexing to measure sensor signals as well as the zero and reference value signals. Each signal will occupy a time slot of approximately 125 milliseconds. Thus all eight signals will be transmitted in a data frame lasting one second. Since only three sensors are used, the data from each will be transmitted twice a second. In order to allow the receiver to separate the signals, the transmitter will insert a frame synchronization interval of 25 milliseconds duration before the zero value signal and a channel synchronization interval of 15 milliseconds before each succeeding channel. During these intervals, a zero-volt level with no AC signal is applied to the sea cable. The receiver can then use missing pulse detectors with appropriate timeout intervals to detect the two synchronizing intervals. The 125-millisecond time slot allows more than adequate timing margins to allow the computer to detect the end of synchronization intervals, measure the signal frequency, and calculate, display and store the results.

The voltage controlled oscillator, (VCO) converts the multiplexed sensor outputs (scattering, temperature, and depth) into a triangle wave which varies in frequency. The voltage to frequency response of the VCO is shown in figure 15. The linearity of the VCO is shown in figure 16. The multiplexed input to the VCO includes both zero and a reference voltage to enable computer correction of data allowing for reasonable variation due to component tolerances or instabilities with time or temperature. This also allows us to make ratiometric measurements.

The timing logic controls timing intervals during which the sensors are connected to the VCO and inserts word and frame synchronization via the FET switch. The line amplifier drives the 500 meter sea cable.



TRANSDUCER PINOUT
SenSym P/N DIV150

| Pin # | Function |
|-------|----------|
| 1 | Ground |
| 8 | -Vout |
| 7 | +Vs |
| 6 | +Vout |

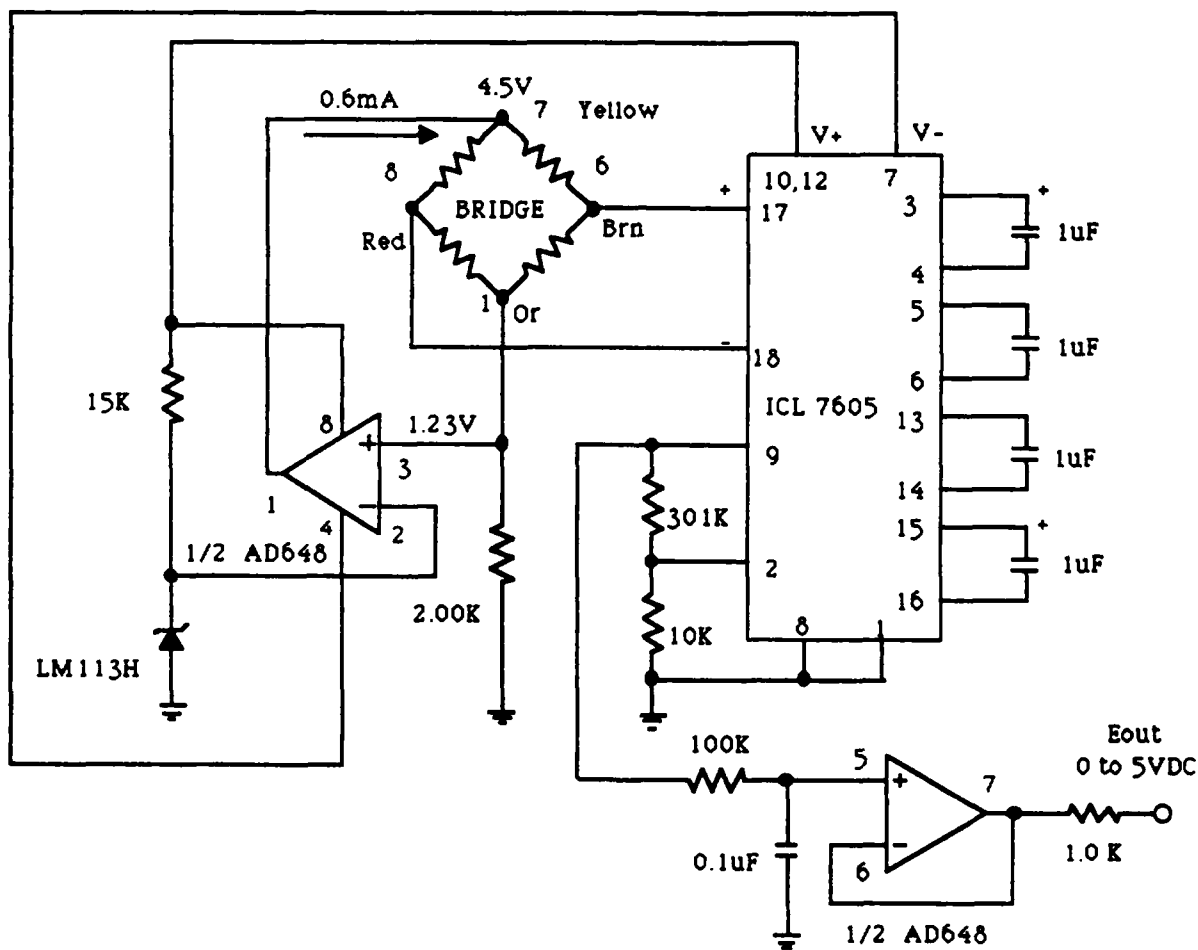


Figure 13, DEPTH SENSOR SCHEMATIC

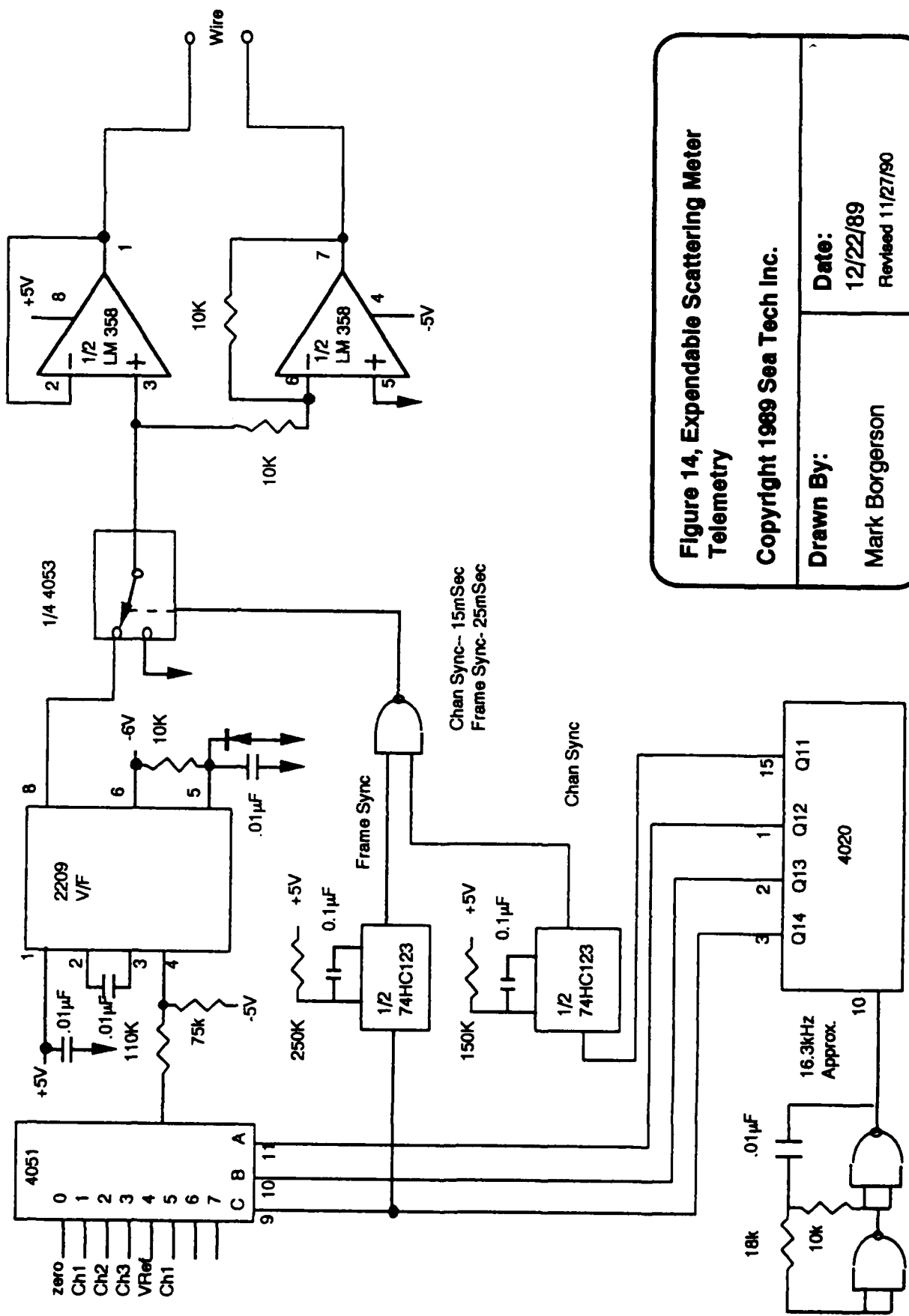


Figure 14, Expendable Scattering Meter Telemetry

Copyright 1989 Sea Tech Inc.

Drawn By:

12/22/89
Revised 11/27/90

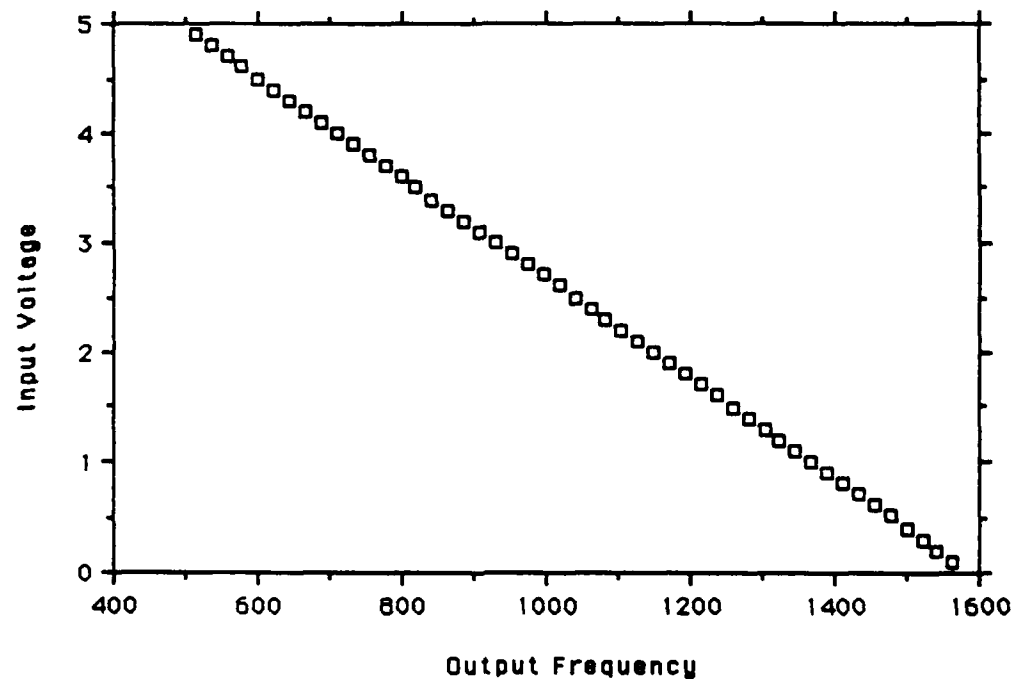


Figure 15, VCO voltage to frequency response

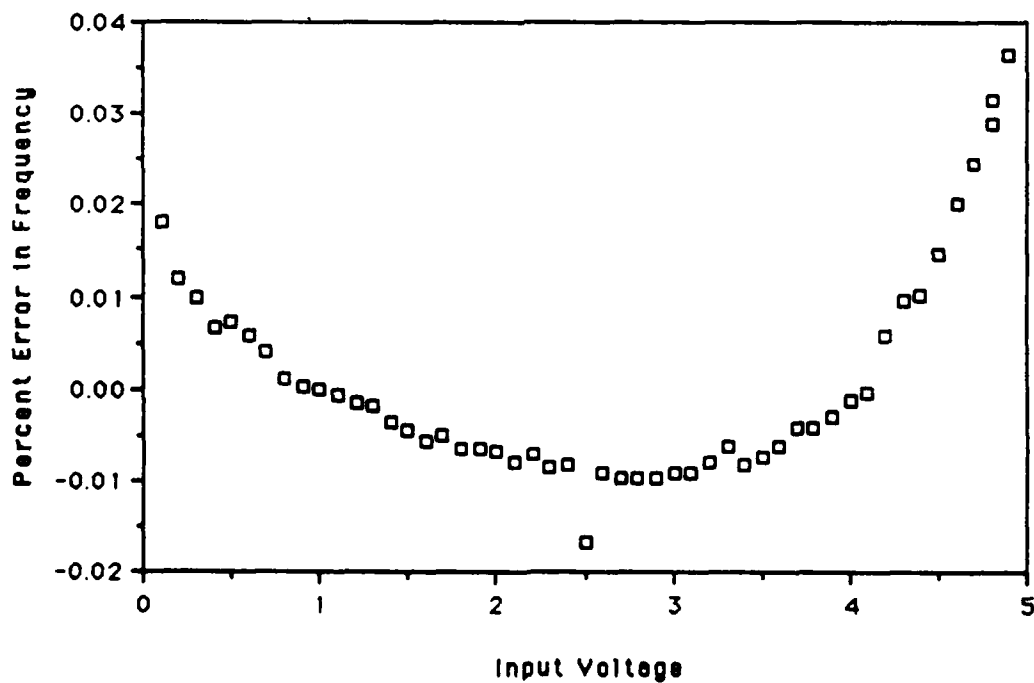


Figure 16, Non-Linearity Errors for the VCO

2f) Sea water switch

A sea water switch will be designed with follow-on funding to apply power to the AXOTD. Laboratory and field tests will be conducted to determine each sensor turn on response time. The design goal will be that all sensor data meet specifications within the first meter of the profile.

2g) Battery power source

The battery will be either a lithium battery with a shelf-life of at least 10 years or an alkaline battery, which has a shorter shelf life but lower cost. An evaluation of tradeoffs between system accuracy, complexity and cost is necessary before a battery selection is made. The lithium battery has more stable voltage discharge characteristics than the alkaline. Shelf life will also be an important consideration because the battery is not used until the seawater switch senses that the unit has entered water. Final battery selection will be determined when system design is finalized.

2h) Sensor housing & weight

The AXOTD housing as shown in figure 17 is 5.5 inches long and 2 inches in diameter. In this space we will package the scattering meter, temperature sensor, depth sensor and their associated electronics. The telemetry electronics, sea water switch electronics and batteries to power the system must also be contained in this space. In addition to all of the above a ballast weight will be designed to obtain a sensor drop rate of 2 m/sec.

2i) Tail fin & wire spool

The tail fin will be used to hydrodynamically stabilize the probe and to house the 500 meter wire spool as shown in figure 17.

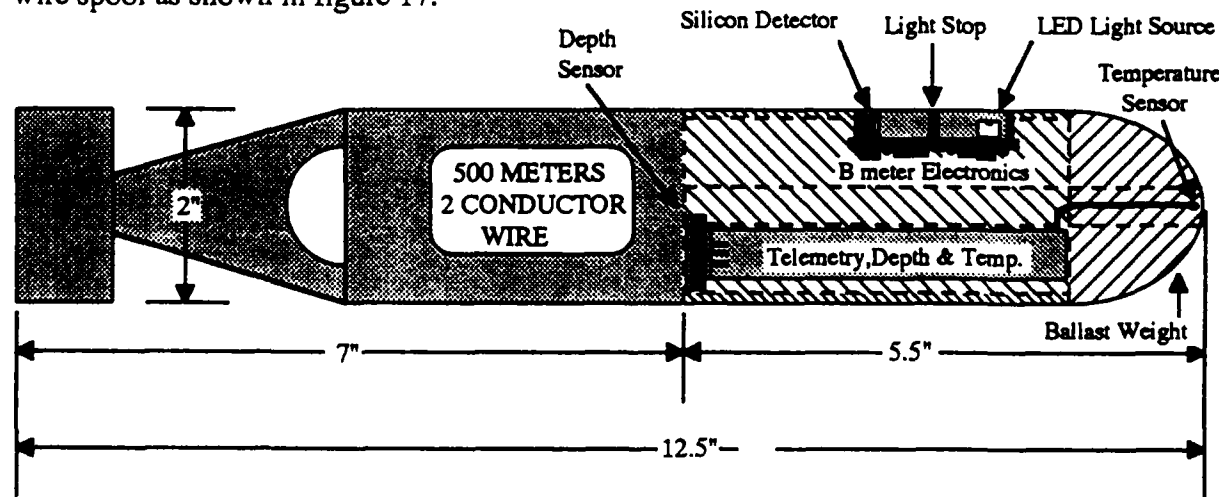


Figure 17, AXOTD conceptual design, 1/2 scale.

3) Computer interface card

The card can be divided into three sections as shown in figure 18, the line receiver, the period counter and the computer interface. All three sections have been designed, prototyped and tested. The line receiver circuitry, period counter and computer interface are shown in Figures 19, 20 and 21.

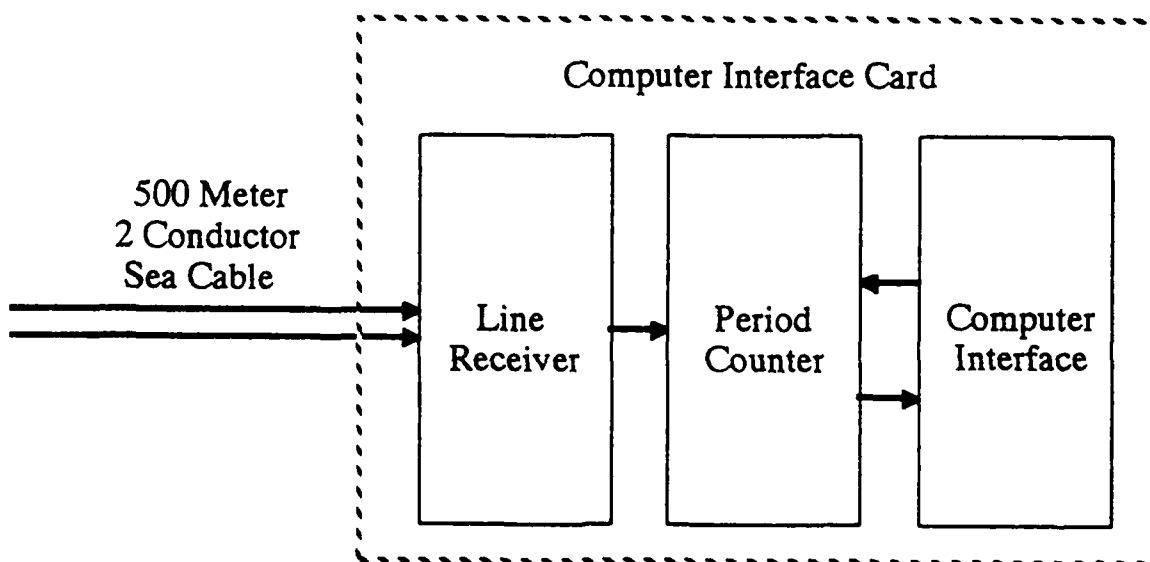


Figure 18, Computer Interface Block Diagram

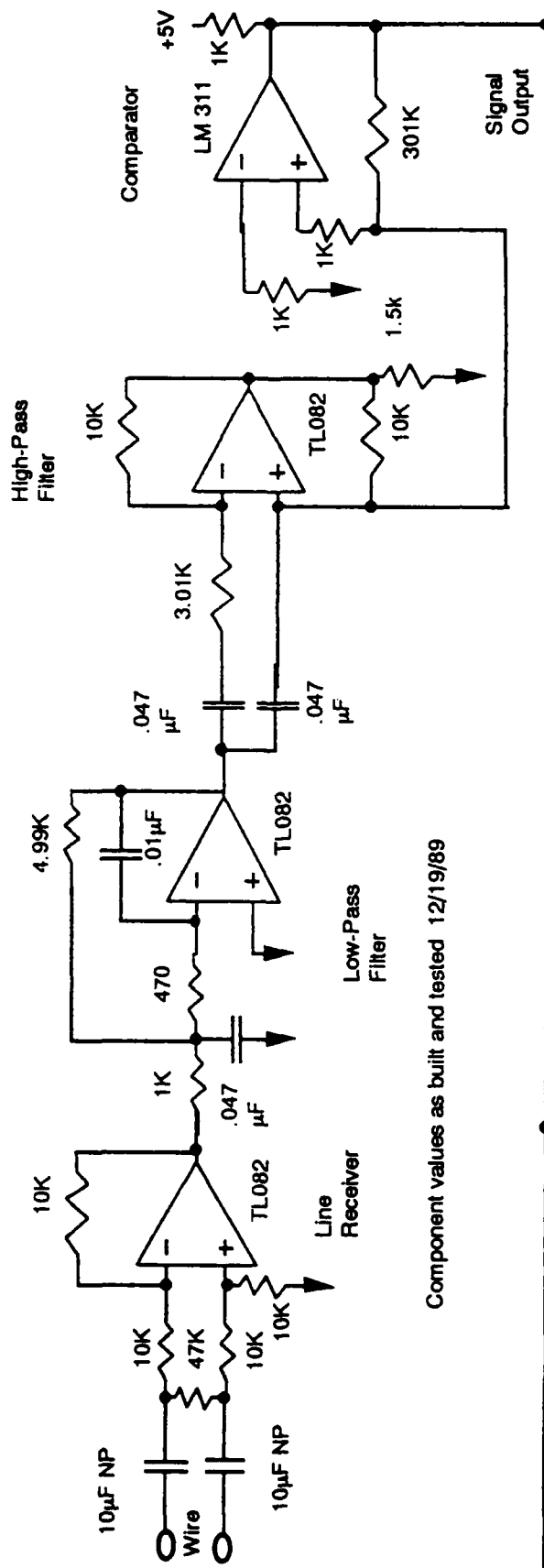
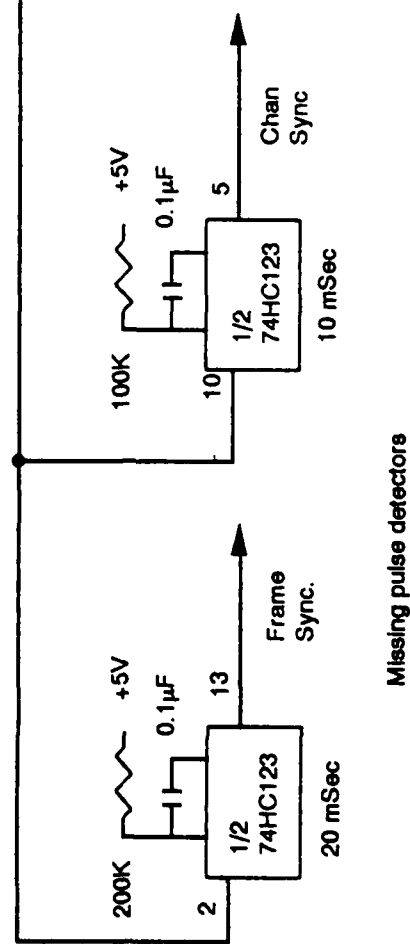
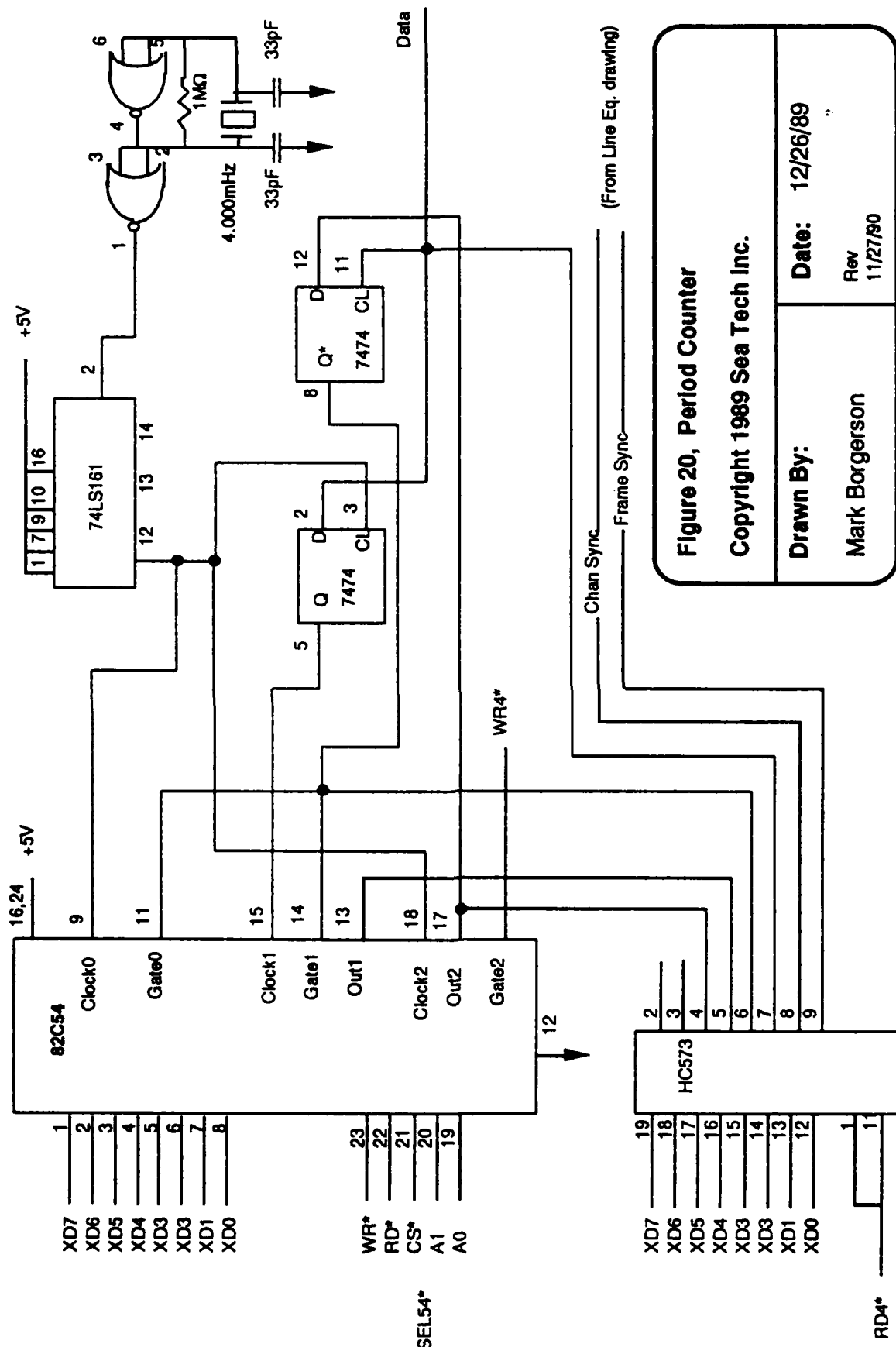


Figure 19, Line Receiver
Line Equalization and Sync Detection
Copyright 1989 Sea Tech Inc.

| | |
|------------------|-----------------------|
| Drawn By: | Mark Borgerson |
| Date: | 12/19/89 |
| | Updated 11/27/90 |





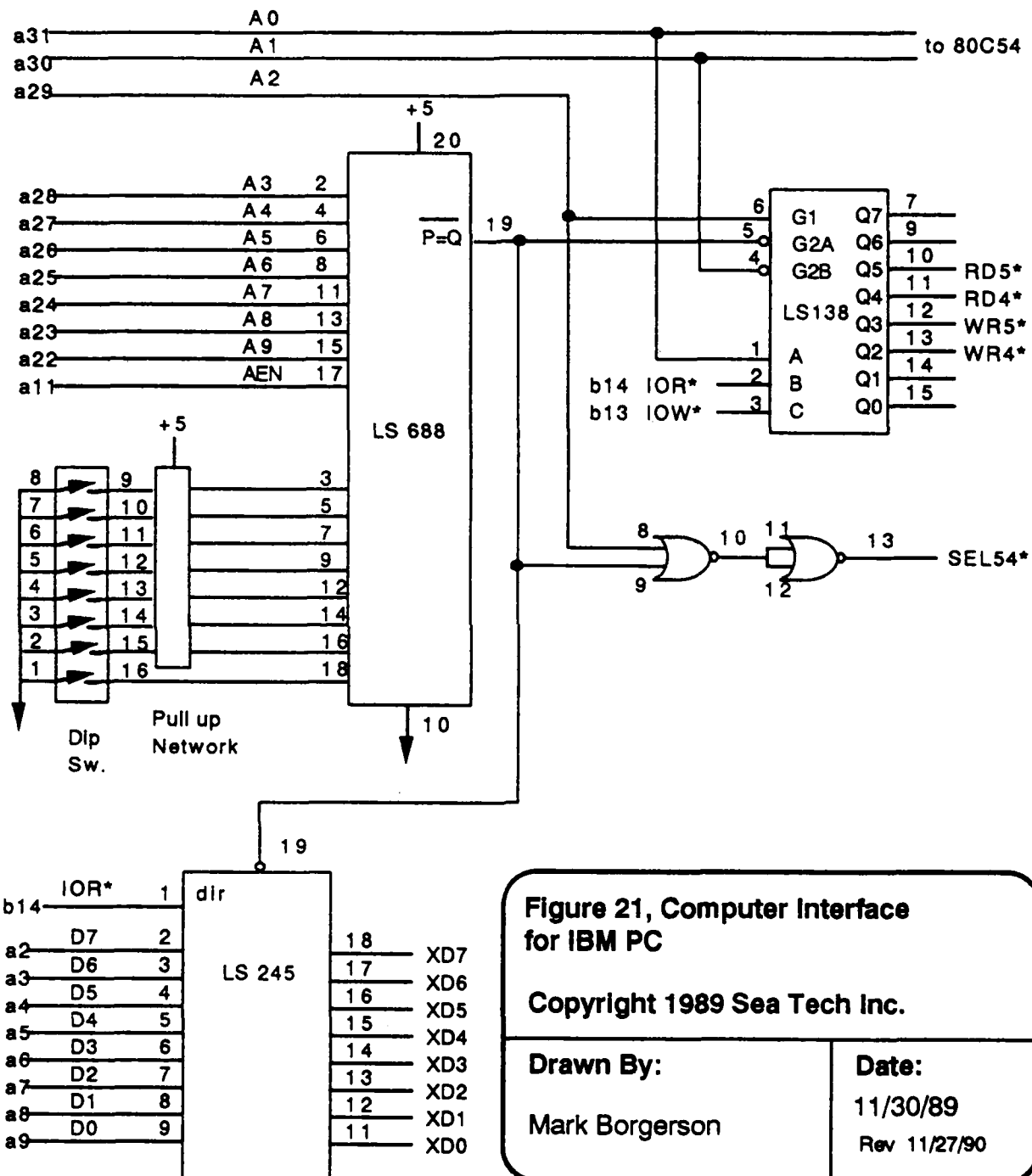


Figure 21, Computer Interface for IBM PC

Copyright 1989 Sea Tech Inc.

Drawn By:

Mark Borgerson

Date:

11/30/89

3a) Line receiver

We have modeled the two wire transmission line and designed a suitable line receiver as shown in figure 19. Transient analysis shows clearly that if one rules out a sine wave then the triangle wave offers the next best approach for data transmission. This receiver was then prototyped and tested with a lumped "line simulator" based on line characteristics shown in figure 11 for the 500 meter sea cable. The receiver consists of a differential amplifier which feeds a low pass / high pass filter and reduces the variation in signal amplitude to about twenty percent of the total signal across the desired frequency range as shown in figure 22.

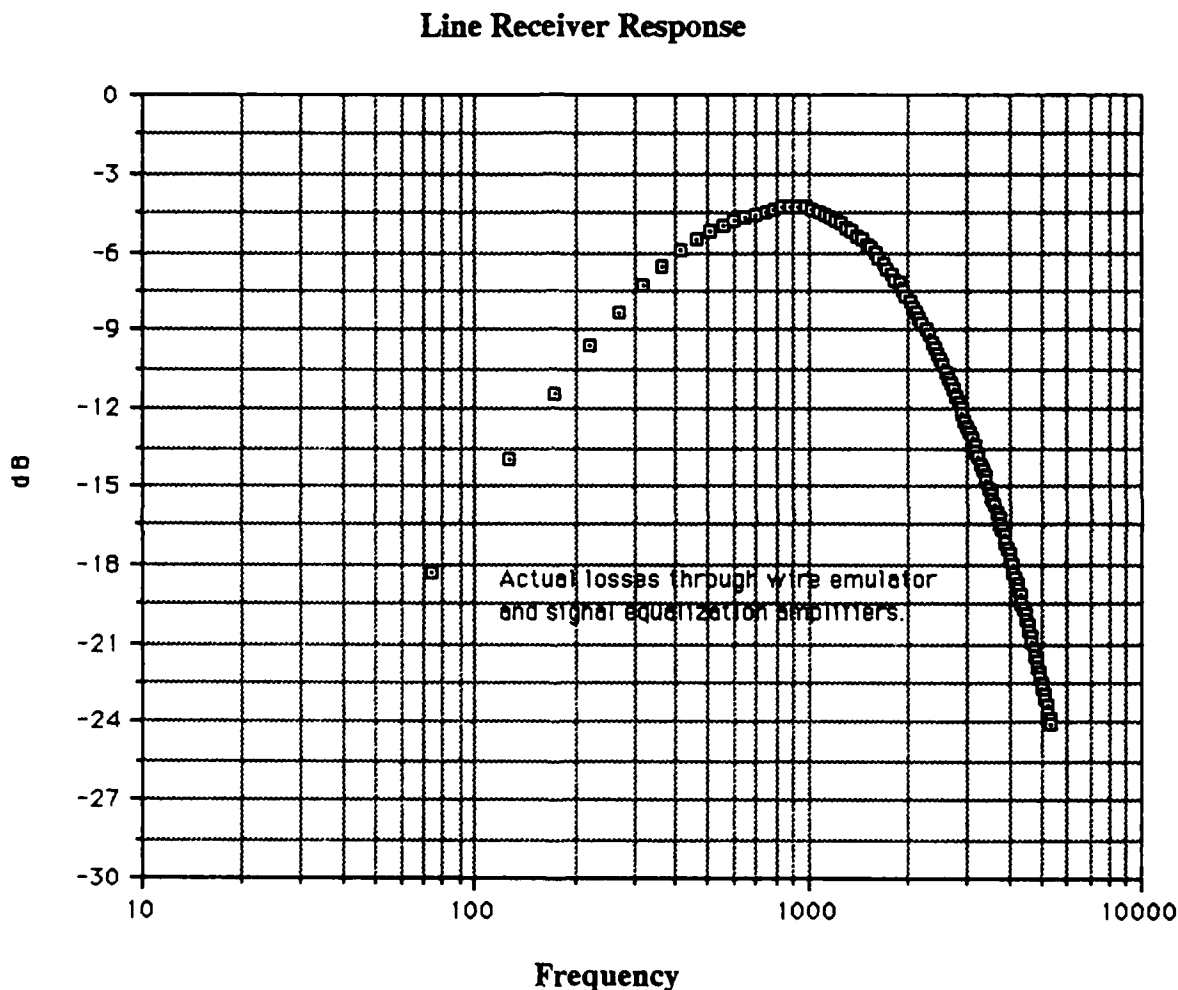


Figure 22, Line receiver frequency response

The line receiver also contains circuitry to detect frame sync and word sync to allow separation of the data from the different sensor channels. The signals from the line receiver are then converted to square waves by a zero-crossing detector and fed to the input of the period counter.

3b) Period counter

The period counter schematic is shown in figure 20. Sensor output is determined by counting the number of square wave pulses from the line receiver in a known time interval. In our prototype, both the data pulses and timing information are collected by a counter-timer integrated circuit. We have designed the software to count the minimum number of pulses whose total period just exceed 66.666 milliseconds. This time interval corresponds to 4 cycles of the 60Hz power line frequency and improves rejection of power-line noise. The exact duration of the input pulses is measured with 2-microsecond resolution. The input frequency is then determined by dividing the number of input pulses by the time. Overall resolution of the system is theoretically 2 microseconds in approximately 66,666, or about one part in 33,333.

3c) Computer interface

The schematic for the computer interface is shown in figure 21. The computer interface was designed to operate with computers of the "IBM™ AT" category. Circuitry to control and read the period counter and transfer data to the computer are included in the computer interface.

4) Computer software

Software has been written to test system performance and is included in appendix A. The software uses word and frame sync to demultiplex the telemetry data. The data is then reduced to engineering units. The zero and reference levels are used to compensate for offset and scale factor errors due to manufacturing tolerances and environmental stability. This technique allows for ratiometric measurements as well, which will simplify sensor design. In the test software, only the data for channel 8 is actually computed and stored. Overall telemetry system noise and linearity as a function of input signals are shown in figure 23. The data shows that more than adequate signal to noise ratio, linearity and accuracy can be achieved with this very simple telemetry system.

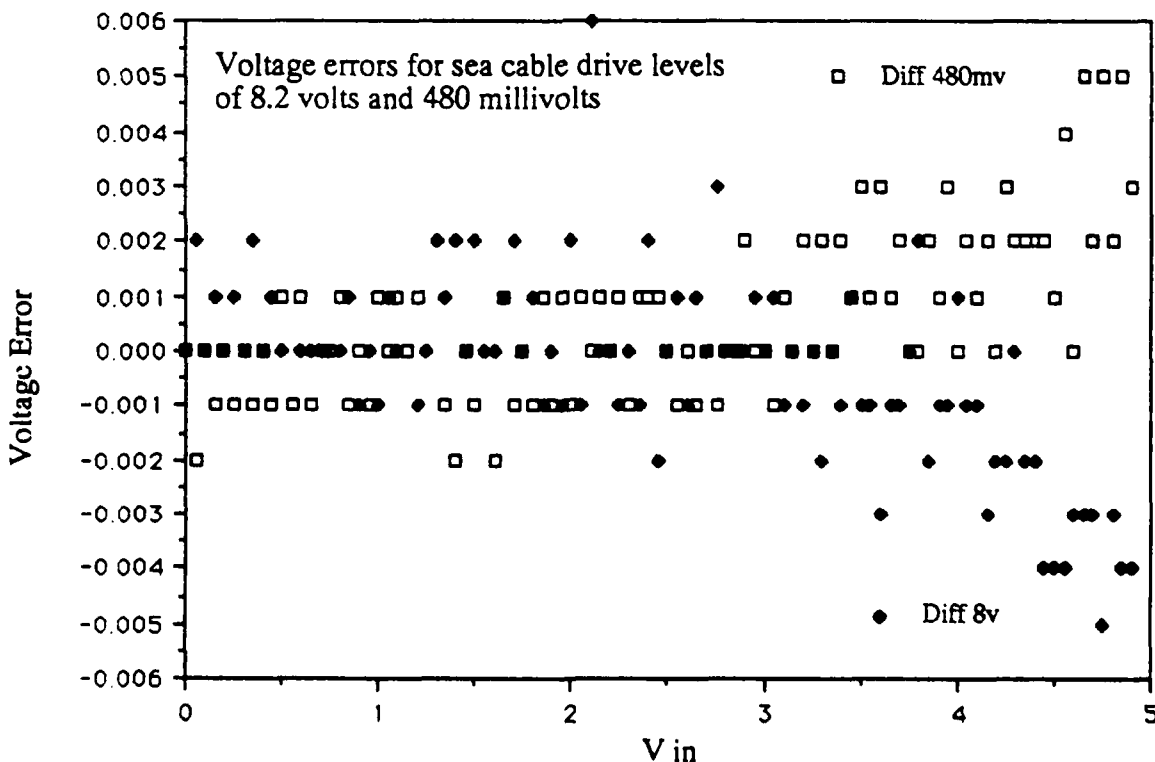


Figure 23. Telemetry System Noise and Linearity

LABORATORY AND FIELD TESTS

Several laboratory tests were conducted to determine the performance of the scattering sensor. These tests addressed the electronic and optical design of the sensor and its sensitivity for the measurement of suspended particulate matter in water.

The scattering sensor was calibrated using a 25 cm transmissometer so that 5 VDC output would correspond to 5 mg/l. Resolution was then determined to be approximately 1 $\mu\text{g/l}$, since electronic noise is less than 1 millivolt RMS. Telemetry noise will degrade this resolution by a factor of 2 for low level signals (figure 23.). Since the natural variability of particulate matter in water is generally much larger than 2 $\mu\text{g/l}$ we initially conclude that the sensitivity of this scattering sensor is adequate to measure particulate matter in both open ocean and coastal waters.

Laboratory and field tests indicates that, when immersed in water, the scattering sensor is not sensitive to ambient sunlight or laboratory lighting. These tests were qualitative in nature; further quantitative testing must be done to document the sensitivity to ambient light.

Laboratory tests in water show that the offset caused by stray or reflected light entering the receiver is reasonably stable and can be corrected by an adjustment procedure during sensor calibration. In this design, ideally, stray or reflected light from the light source will not enter the receiver, so that the absence of particles in water will result in zero output. Practically, a small amount of light is scattered in particle free water causing a zero offset. The problems related to zero offset, i.e. molecular scattering, wall effects, and reflections in general need to be further evaluated. Since stability of the zero offset will limit sensor accuracy, this parameter will be extensively evaluated during the proposed NOARL research effort..

Temperature stability of the scattering sensor, as well as long term stability, has not been evaluated. These parameters will be addressed during the next phase of the research.

Laboratory tests were conducted in a large, well stirred tank to determine the response of the scattering sensor to suspended particulate matter in water. The beam attenuation coefficient was measured using a Sea Tech 25 cm transmissometer. Sensitivity and dynamic range were determined using biologically active pond water and dilutions of bottom mud samples from 5000 m depth off Nova Scotia collected during the HEBBLE experiment. The results are shown in Figure 24 and Figure 25. For each type of particulate matter the scattering was very linear with beam attenuation. The scattering sensor was at least as sensitive as the transmissometer as shown by the slopes of 0.91 and 1.68 in Figure 24.

Since the sensitive volume of the scattering sensor is much smaller than that of the transmissometer, a natural question to ask is: how noisy is the scattering sensor output relative to the 25 cm transmissometer in a well stirred tank containing suspended particulate matter. The electronic time constant for the scattering sensor is 1 second. The transmissometer time constant is 0.1 second. Figure 25 shows the RMS signal levels for both the scattering sensor and transmissometer. This data shows that environmental noise is highly correlated with signal level for the scattering sensor as one would expect. The high environmental noise for the scattering sensor is due to its smaller sample volume. The transmissometer has much lower RMS signal levels since it has a much larger sensitive volume.

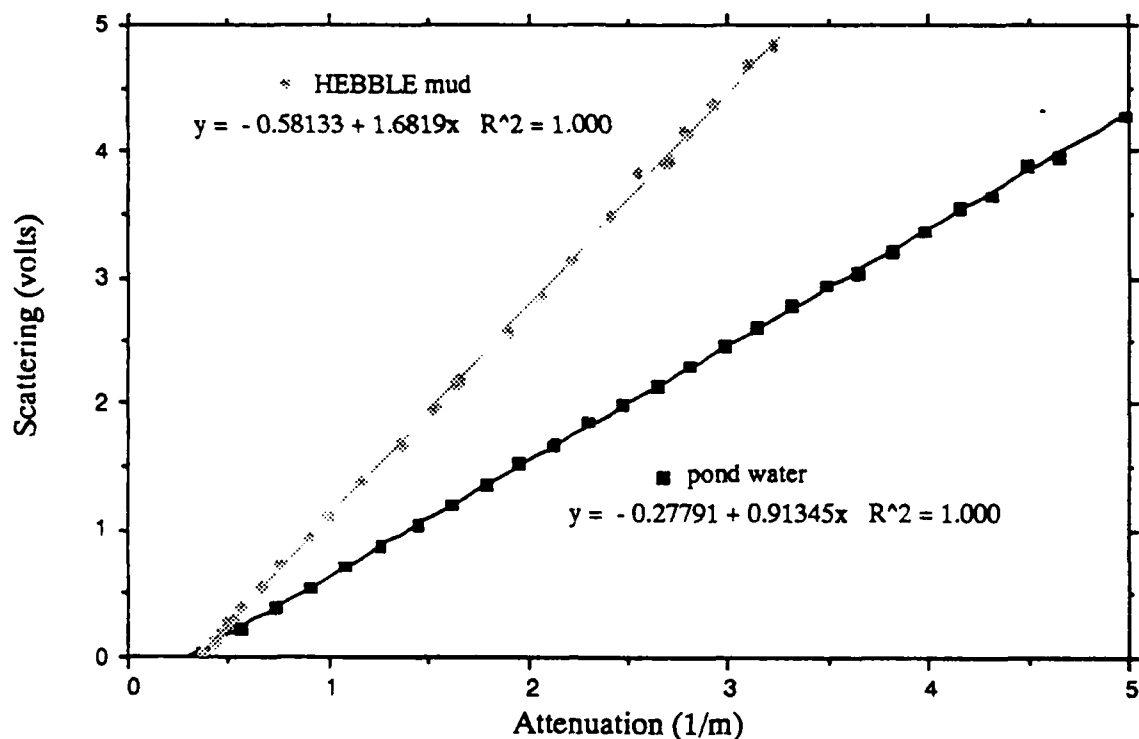


Figure 24. Scattering sensor output versus beam attenuation for dilutions of HEBBLE mud and pond water.

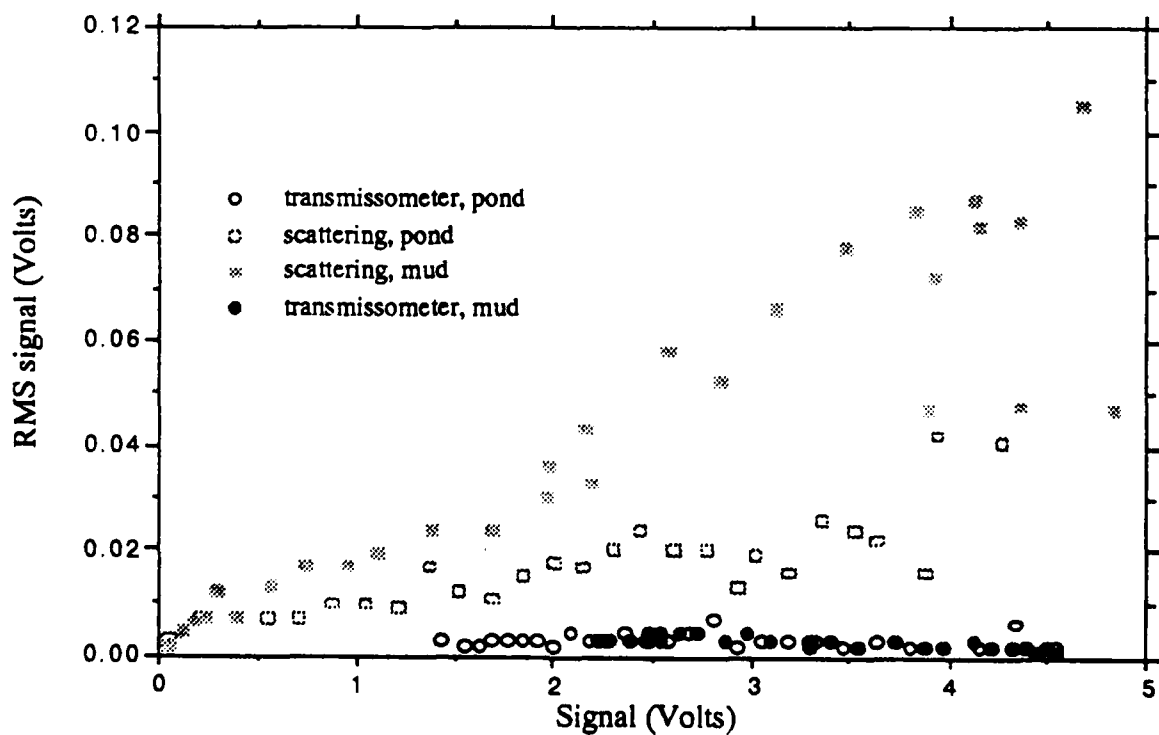


Figure 25. Variability of scattering sensor and transmissometer output as a function of particle concentration..

We tested the prototype expendable scattering sensor (650 nm, Figure 5) at sea on August 14, 1990. Casts were made at two stations; one at 5 NMi and one at 10 NMi from Newport, Oregon. In addition to scattering, we measured profiles of temperature and beam attenuation (660nm) as a function of depth. Following are the profiles (Figures 26 and 27) for casts at both stations and plots of scattering versus attenuation at both stations (Figures 28 and 29). Note the extremely high, depth-segmented correlation between scattering and attenuation ($r^2 \sim 0.95$). There are two scattering-to-attenuation ratios for Station 1, which are repeated in Station 2 with the addition of another ratio. The three relationships represent the surface layer, the mid-depth turbidity minimum layer and the bottom nepheloid layer. Since the inshore surface slope was similar to the offshore mid-depth slope, we probably observed the two-cell coastal upwelling circulation pattern described by Mooers et al., 1976. The large difference in the nature of surface populations onshore and offshore of the resulting front are reported by Kitchen et al. (1978).

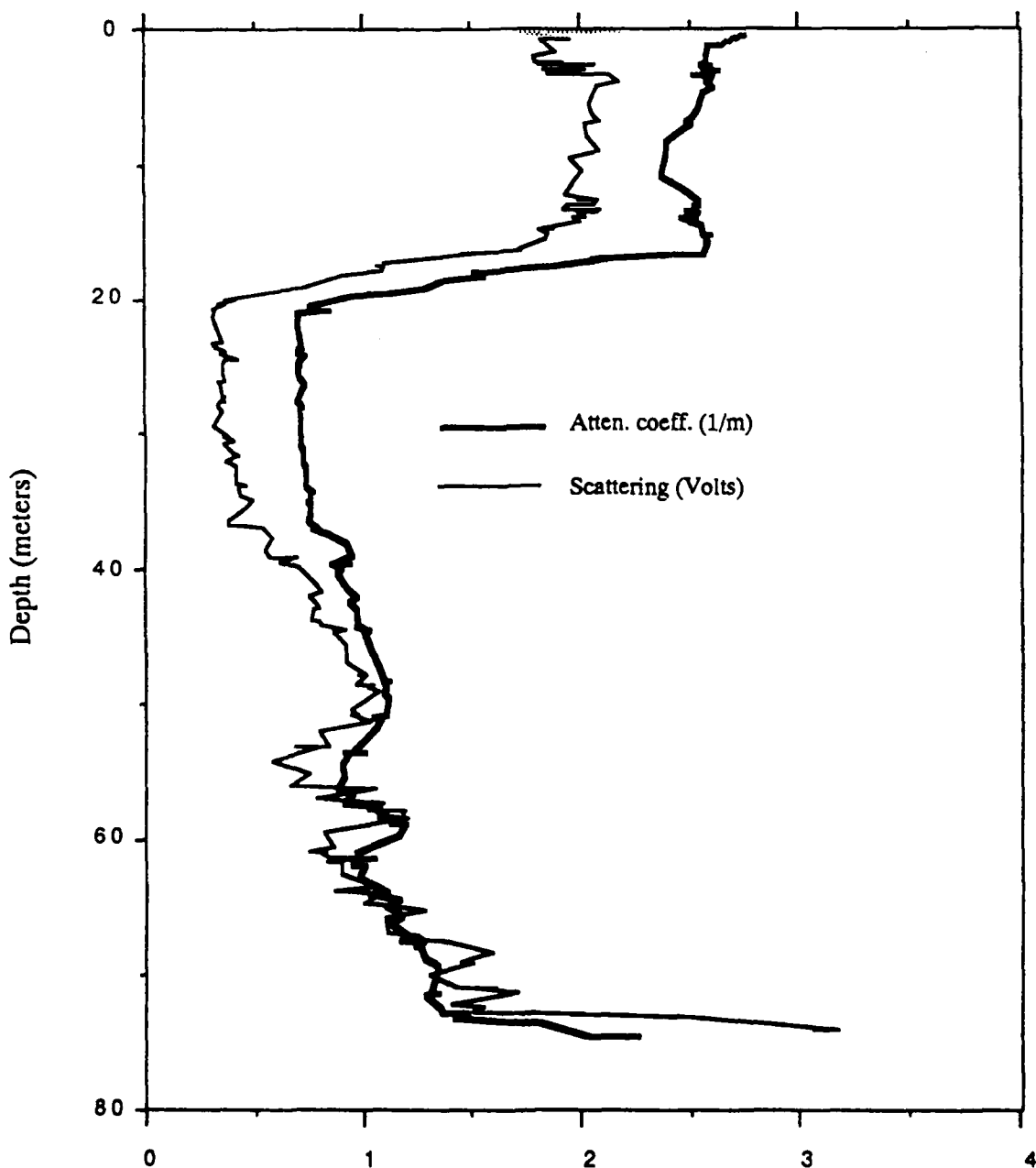


Figure 26, Station 1, 5 NMi west of Newport Oregon

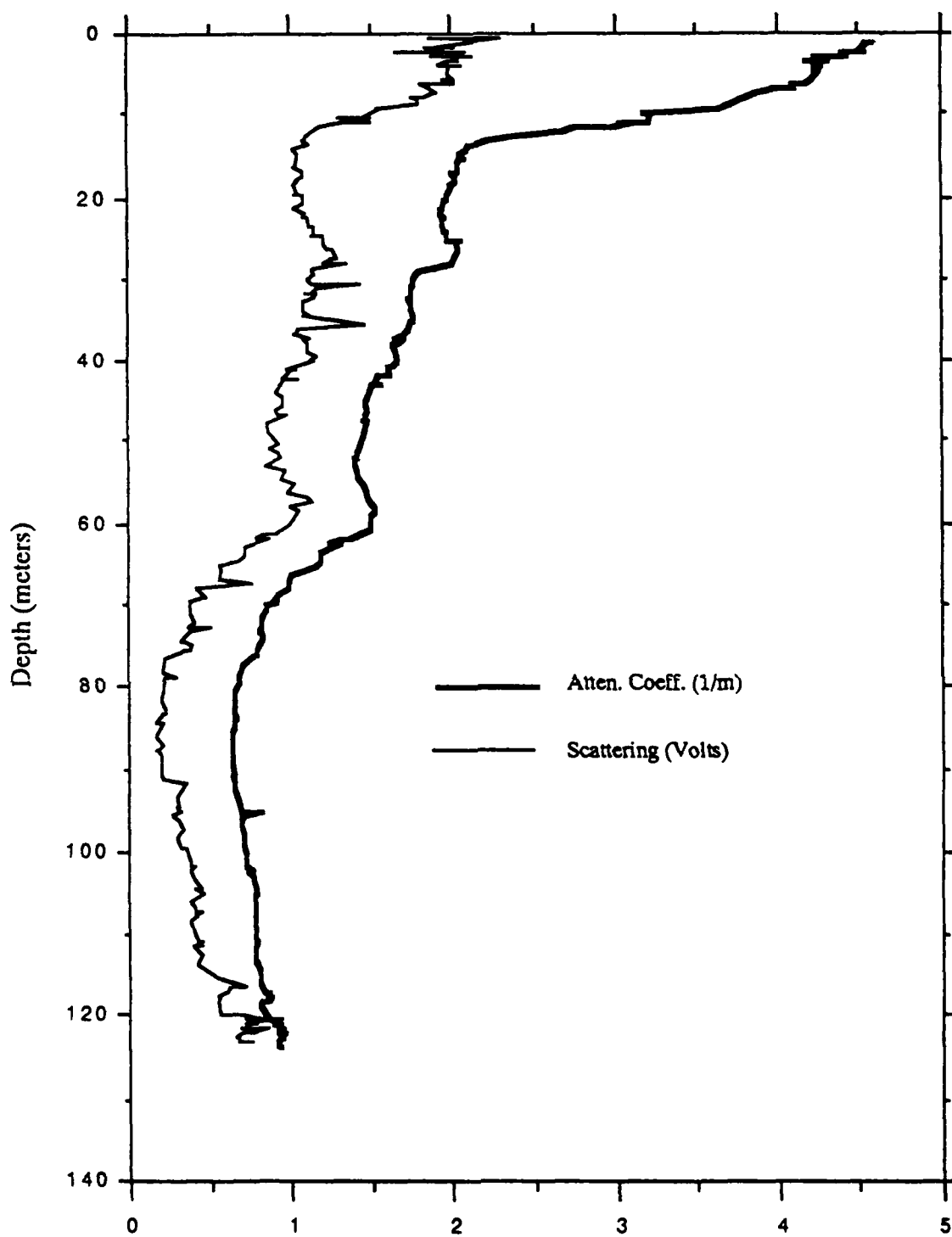


Figure 27. Station 2, 10 NMi west of Newport, Oregon

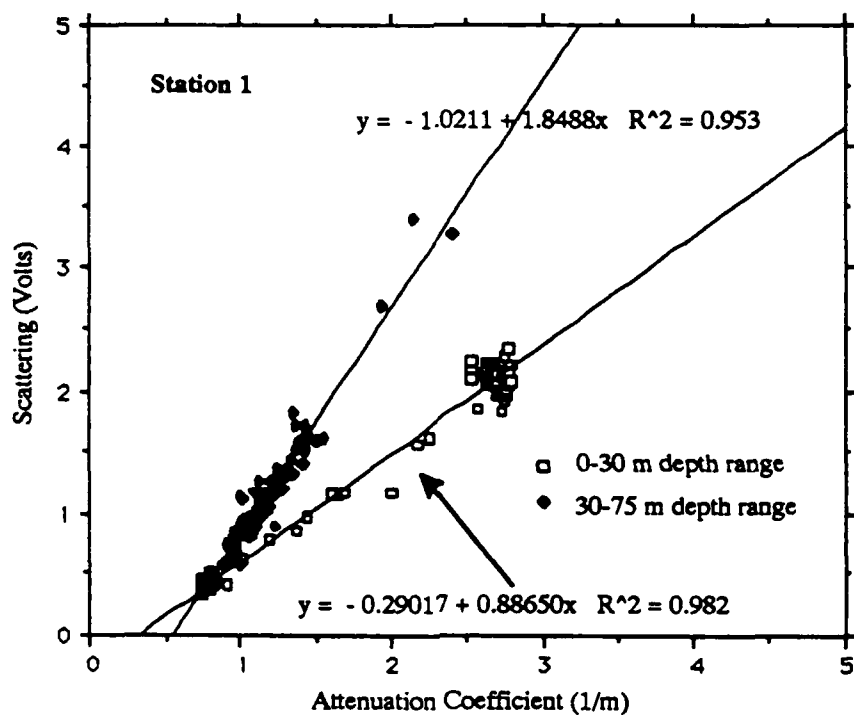


Figure 28. Segmented correlation between scattering and attenuation coefficient at station 1, 5 NMi west of Newport Oregon

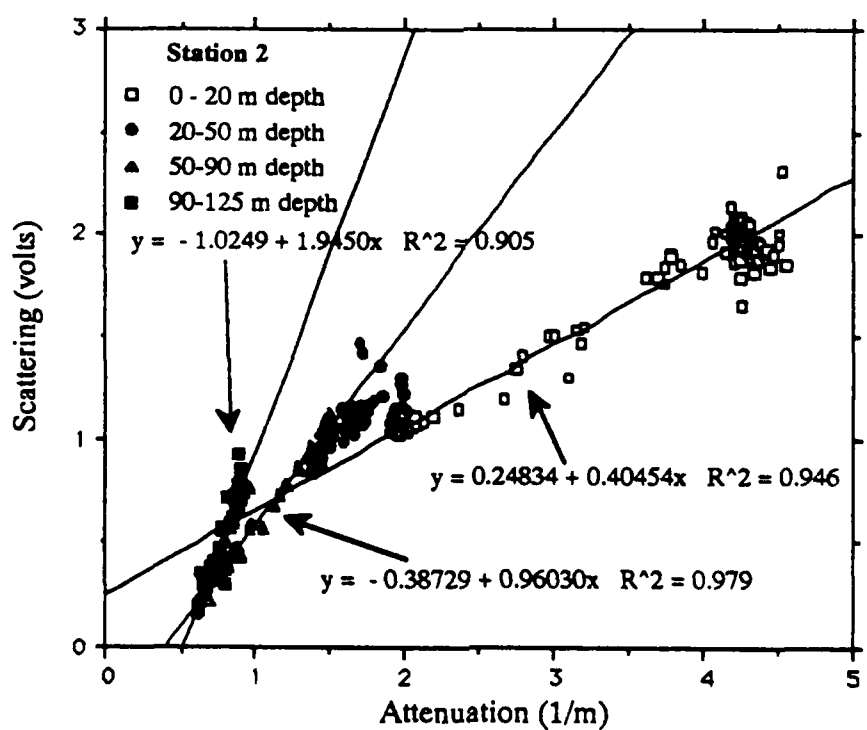


Figure 29. Segmented correlation between scattering and attenuation coefficient at station 2, 10 NMi west of Newport Oregon

The NOARL expendable particle sensor was further tested during a cruise off San Diego on November 14, 1990. Ten stations were taken, primarily to test new designs of a transmissometer and absorption meter at 488 nm, corroborating data consisting of transmission at 660 nm, CTD, fluorescence, and light scattering at 650 nm were also taken. The water was very clean. Dr. Mueller of CHORS- SDSU indicated that El Nino -like water had penetrated the area, identified by tropical flora and fauna. This happened even though no large scale El Nino is occurring. The clear water provided an ideal test for the scattering sensor in very clean natural water.

A comparison of the profiles of light scattering at 650 nm and beam attenuation at 660 nm (figure 30) are shown for the clearest station of the day, station 9. The entire range of particle concentration (based on beam attenuation) was about $70 \mu\text{g/l}$. This is less than twice the particulate matter range in the Sargasso Sea.

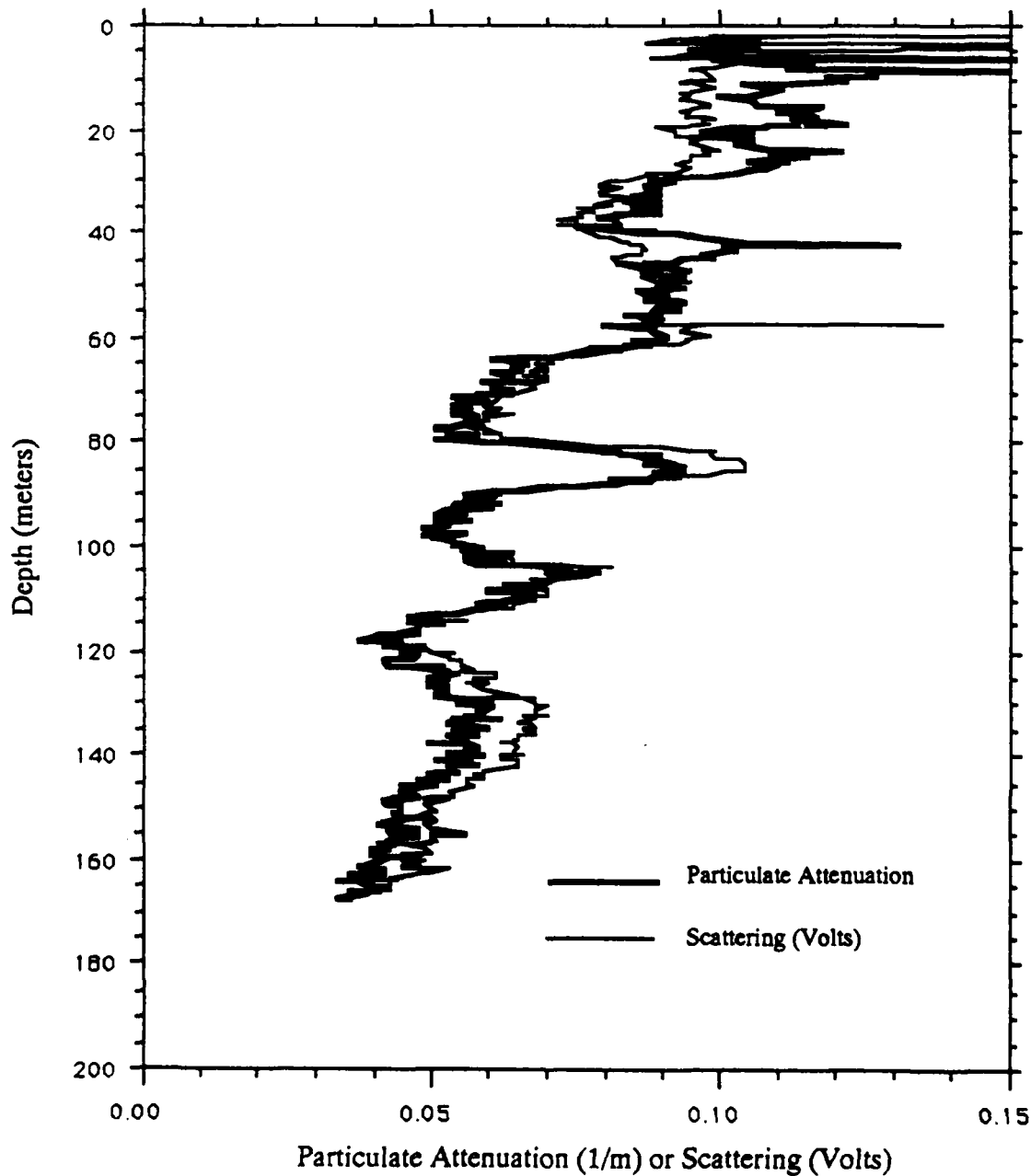


Figure 30. Profile of Particulate Attenuation and Scattering at Station 9 off San Diego, California.

Note that the scattering and attenuation in figure 30 match very well feature by feature, but that on the whole the scattering decreases more slowly as a function of depth. This is probably caused by an increase in the scattering sensor LED power output as temperature decreases with depth. The scattering sensor LED power output has a negative temperature coefficient of approximately 1% / °C. Note also that this temperature effect is evident in the profiles taken off Newport, Oregon, figures 26 and 27. Since the AXOTD will measure water temperature, we plan to correct for the LED temperature coefficient in the data reduction process using software. This problem will be further addressed during future research.

Figure 31 shows the light scattering as a function of particulate attenuation for station 9 off San Diego, California. The water below 60 meters shows a high linear correlation between scattering and attenuation. This relation is probably due to dilutions of one kind of resuspended sediment (the station was taken only 4 miles from the Coronado Islands). Above 60 meters the correlation is much poorer, due to a much smaller dynamic range in parameters, and due to the presence of organic matter. Organic matter is expected to show a change in the scattering-to-attenuation ratio due to photo-adaptation. In addition the phytoplankton assemblage may change as a function of depth.

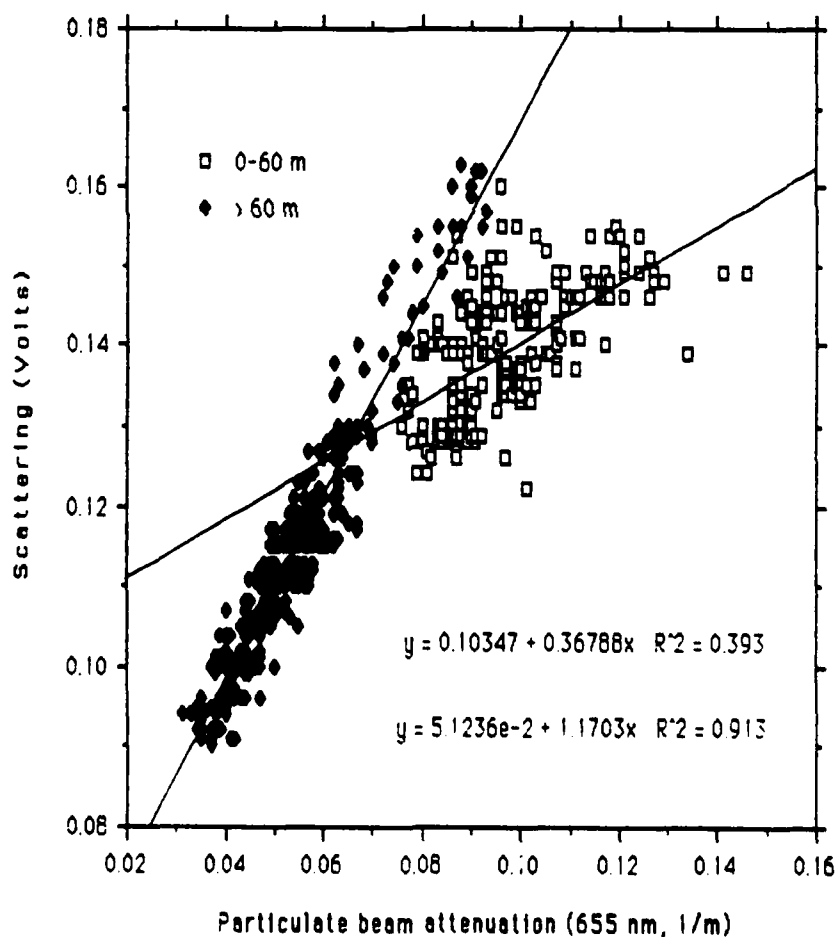


Figure 31. Light Scattering vs Particle Attenuation at Station 9 off San Diego

RELATED WORK

Further development and evaluation of expendable scattering sensors were completed with funding from the Office of Naval Research. Results from this additional work are described in a final report to the Office of Naval Research.

REFERENCES

Bartz, R., J. R. V. Zaneveld and H. Pak (1978) A transmissometer for profiling and moored observations in water, *Ocean Optics V, Proc. Soc. Photo Opt. Instrum. Eng.*, **160**, 102-108.

Bricaud, A., A. Morel and L. Prieur (1983) Optical efficiency factors of some phytoplankters. *Limnol. Oceanogr.* **28**: 816-832.

Jerlov, N. G. (1976) *Marine Optics*. Elsevier, Amsterdam, 231 pp.

Kitchen, J. C., J. R. V. Zaneveld and H. Pak (1978) The vertical structure and size distributions of suspended particles off Oregon during the upwelling season. *Deep-Sea Res.*, **25**, 453-468.

Kitchen, J. C., J. R. V. Zaneveld and H. Pak. (1982) Effect of particle size distribution and chlorophyll content on beam attenuation spectra. *Appl. Opt.*, **21**, 3913-3918.

Mie, G. (1908) Beiträge zur Optik trüber Medien, speziell kolloidalen Metall-lösungen, *Ann. Phys.*, **25**, 377.

Mooers, C. N. K., C. A. Collins and R. L. Smith (1976) The dynamic structure of the frontal zone in the coastal upwelling region off Oregon. *J. Phys. Oceanogr.*, **6**, 3-21.

Morel, A. (1973) Diffusion de la lumière par les eaux de mer. Résultats expérimentaux et approche théorique. In: *Optics of the Sea*. AGARD lecture series **61**, pp. 31.1-31.76.

Postel, J. R., W. K. Peterson, J. C. Kitchen and D. W. Menzies (1980) Data report of the DOE-sponsored Northwest Marine Sciences Group July-August 1979 cruise. Dept. of Oceanography, University of Washington Ref. A80-37, 453 pp.

Spinrad, R. W. (1986) A calibration diagram of specific beam attenuation. *J. Geophys. Res.* Vol 91, No C6 7761-7764

Spinrad, R. W., J. R. V. Zaneveld, and J. C. Kitchen (1983). A study of the optical characteristics of the suspended particles in the benthic nepheloid layer of the Scotian Rise. *J. Geophys. Res.* Vol 88, No C12 7641- 7645.

Zaneveld, J. R. V. (1973) Variation of optical sea parameters with depth. AGARD-NATO lecture series No. 61 *Optics of the Sea*, AGARD-LS-61, pp 2.3-1 through 2.3-22.

Appendix A

```

Program SWPExp;
{test response of expendable telemetry system }
{receive results through com2 at 9600 baud}
{M. Borgerson
USES DOS, CRT;

const
  DIOBase      = $218;      {Data I/O 2811PGH base Address}
  DacBase      = $21A;      {DAC output address}
  ADCSR        = $218;
  ADCCHGain   = $219;
  ADCData      = $21A;
  cycleTime    = 10;        {milliseconds per output cycle}
  maxtime      = 100.0;     {runs for 100 seconds}

var ch:char;
    time,v1,v2, period: real;
    infile,outfile:text;
    involts1,involts2: real;
    outfileName:string;
    ioErr,i: integer;

{Set DAC 0 output to voltage v}
Procedure Dac0Out(v:real);
var pWord: word;
Begin
  pWord:= round((v+5.000)*409.6);
  portw[dacbase]:= pword and $FFF;
END;

{Set DAC 1 output to voltage v}
Procedure Dac1Out(v:real);
var pWord: word;
Begin
  pWord:= round((v+5.000)*409.6);
  portw[dacbase+2]:= pword and $FFF;
END;

Procedure SetCom2Speed;
var r:registers;
Begin
  r.ah:= 0;
  r.al:= $E3; {9600, n,8,1}
  r.dx:= 1; {com 2}
  intr($14,r);
End;

```

```

Begin {SWPEXP program}
  time:= 0.0;
  v1:= 0.0;
  v2:= 0.0;
  Clrscr;

  Write('Output File Name: ');
  Readln(outfileName);
  Assign(outfile, outfile);
  Rewrite(outfile);
  Assign(infile, 'COM2');
  Reset(infile);
  SetCom2Speed;
  Writeln('Beginning sweep cycle');
  Dac0out(v1);
  {$I-}
  for i:= 1 to 5 do
  Begin
    readln(infile);
    ioerr:= ioreresult;
  end;

  {$I+}
  While v1 < 4.95 do
  Begin
    {$I-}
    Repeat
      Readln(infile,involts1,involts2);
      ioErr:= ioreresult;
      If ioerr <> 0 then Writeln(ioerr);
      Readln(infile,involts1,involts2);
      ioErr:= ioreresult;
      If ioerr <> 0 then Writeln(ioerr);
    until ioerr = 0;
    {$I+}
    Writeln(v1:8:3,involts1:8:3,involts2:8:3);
    Writeln(outfile,v1:8:3,chr(9),involts1:8:3,
            chr(9),involts2:8:3);
    v1:= v1+0.050;
    Dac0out(v1);
    If keypressed then exit;
  End;
  Close(infile);
  Close(outfile);
  Writeln('Test complete');
End

```

```

Program Exptest;
{program to test interface to expendable scattering meter}
{this program collects frequency data from the prototype}
{card and sends it to another computer via RS232 serial}
{port This allowed us to test the prototype in an old, cheap}
{PC clone, while using a more expensive and capable computer}
{to generate the frequency data and collect the results}
Uses DOS, CRT;
const
  iobase = $340;
  ctlReg = iobase+3;
  statByte = iobase+4;
var ch: char;
  bt:byte;
  i,j:word;
  infreqs,involts:array[1..8] of real;
  fname:string;
  outfile:text;
Procedure SetGateTime(counts:word);
Begin
  port[ctlreg]:= $B2; {sets mode 1}
  Delay(3);
  Port[iobase+2]:= counts and 255;
  port[iobase+2]:= (counts div 255);
End;

Function Freq: Real;
var th,tl:byte;
  tcount,incount:word;
  ctime:real;
Begin
  port[ctlreg]:= $30;{set time counter 0 for mode 0}
  Delay(1);
  port[iobase]:= 0; {set initial count to 0000}
  port[iobase]:= 0;
  {now set up the input counter}
  port[ctlreg]:= $70; {counter 1 to mode 0}
  Delay(1);
  port[iobase+1]:= $0;
  port[iobase+1]:= $0;

  {now open the gate for preset time}
  port[iobase+4]:=0; {trigger the count}
  Delay(10); {wait for gate to open}
  repeat until (port[statbyte] and 8)=0; {wait for gate to close}
  tl:= port[iobase];
  th:= port[iobase]; {read the count—gate is closed}
  tcount:= 65536-(th*256+tl);
  ctime:= 1.99962*tcount;
  tl:= port[iobase+1]; {read low count from input}
  th:= port[iobase+1];
  incount:= 65536-(th*256+tl);
  If ctime > 0 then
    freq:= incount/ctime*1e6
  else freq := 5000;
End;

```

```

Procedure ChanSync;
var stime:integer;
Begin
  stime:= 0;
  Repeat until (port[statbyte] and 2)=0; {wait for sync low}
  Repeat
    inc(stime);
    Delay(1);
  until (port[statbyte] and 2)=2; {wait for sync high}
end;

Procedure FrameSync;
var stime:integer;
Begin
  stime:= 0;
  Repeat until (port[statbyte] and 1)=0; {wait for frame sync low}
  Repeat
    inc(stime);
    Delay(1);
  until (port[statbyte] and 1)=1; {wait for sync high}
end;
Procedure ReadFreqs;
var i: integer;
Begin
  FrameSync;
  for i:= 1 to 7 do
  Begin
    infreqs[i]:= freq;
    If (infreqs[5] <> infreqs[1]) then
      involts[i]:= 2.5158*(infreqs[i]-
      infreqs[1])/(infreqs[5]-infreqs[1]);
    ChanSync;
  End;
  infreqs[8]:= freq;
  If (infreqs[5] <> infreqs[1]) then
    involts[8]:= 2.5158*(infreqs[8]-infreqs[1])/(infreqs[5]-
    infreqs[1]);
  End;

Procedure WriteResults;
var i:integer;
Begin
  Gotoxy(1,5);
  for i:= 1 to 8 do
  Begin
    Write(infreqs[i]:8:2);
  End;
  Gotoxy(1,6);
  for i:= 1 to 8 do
  Begin
    Write(invols[i]:8:3);
  End;

```

```
Procedure SetAuxSpeed;
var r:registers;
Begin
  r.ah:= 0;
  r.al:= $93; {1200,n,8,1}
  r.dx:= 0;
  Intr($14,r);
End;

Begin
  SetGateTime(33333);
  Clscr;
  ch:= ' ';
  Write('output file name? ');
  Readln(fname);
  for i:= 1 to length(fname) do
    fname[i]:= Uppcase(fname[i]);
  {
  If (fname = 'AUX') or (fname = 'COM1') Then SetAuxSpeed;
  }
  assign(outfile,fname);
  Rewrite(outfile);
  repeat
    ReadFreqs;
    WriteResults;
    {$I-}
    Writeln(outfile,involts[2]:8:3,chr(9),involts[3]:8:3);
    Writeln(outfile,involts[6]:8:3,chr(9),involts[7]:8:3);
    i:= iorestult;
    {$I+}
    If keypressed then ch:= readkey;
  until ch='q';
  close(outfile);
End.
```